

Review

# Preparation, Characterization and Application of Polysaccharide-Based Metallic Nanoparticles: A Review

Cong Wang, Xudong Gao, Zhongqin Chen, Yue Chen and Haixia Chen \*

Tianjin Key Laboratory for Modern Drug Delivery & High-Efficiency, School of Pharmaceutical Science and Technology, Tianjin University, Tianjin 300072, China; 1015213012@tju.edu.cn (C.W.); xdgao@tju.edu.cn (X.G.); chenzhongqin@tju.edu.cn (Z.C.); chen Yue0126@tju.edu.cn (Y.C.)

\* Correspondence: chenhx@tju.edu.cn; Tel.: +86-22-2740-1483

Received: 8 November 2017; Accepted: 5 December 2017; Published: 8 December 2017

**Abstract:** Polysaccharides are natural biopolymers that have been recognized to be the most promising hosts for the synthesis of metallic nanoparticles (MNPs) because of their outstanding biocompatible and biodegradable properties. Polysaccharides are diverse in size and molecular chains, making them suitable for the reduction and stabilization of MNPs. Considerable research has been directed toward investigating polysaccharide-based metallic nanoparticles (PMNPs) through host–guest strategy. In this review, approaches of preparation, including top-down and bottom-up approaches, are presented and compared. Different characterization techniques such as scanning electron microscopy, transmission electron microscopy, dynamic light scattering, UV-visible spectroscopy, Fourier-transform infrared spectroscopy, X-ray diffraction and small-angle X-ray scattering are discussed in detail. Besides, the applications of PMNPs in the field of wound healing, targeted delivery, biosensing, catalysis and agents with antimicrobial, antiviral and anticancer capabilities are specifically highlighted. The controversial toxicological effects of PMNPs are also discussed. This review can provide significant insights into the utilization of polysaccharides as the hosts to synthesize MNPs and facilitate their further development in synthesis approaches, characterization techniques as well as potential applications.

**Keywords:** biopolymers; polysaccharides; polysaccharide-based metallic nanoparticles; host–guest strategy; preparation and characterization; application; toxicity evaluation

## 1. Introduction

Scientific research on nanotechnology has received tremendous interest in this century due to its interdisciplinary applications in the field of catalysis, biomedicine, fuel cells, magnetic data storage and energy technology [1]. Nanoparticles (NPs), with the size range from 10.0 to 100.0 nm in diameter, have unique features including high surface area, quantum property as well as adsorption and releasing properties, exhibiting great potential in multifunctional applications [2]. Among all nanoparticles, metallic nanoparticles (MNPs) are especially attractive owing to their unique properties and diverse applications [3]. It has been accepted that the size, morphology, dispersibility and physicochemical properties of MNPs are strongly associated with their applications, which are affected by the synthesized approach [4]. Thus, the investigations of searching new hosts for controlling the properties of MNPs have been one of the main objectives in MNPs research [5]. Moreover, conventional synthesis techniques of MNPs are chemicals and energy consuming, causing various risks to the environment [6]. The awareness of developing an alternatively green synthesis approach is evolving into another objective in MNPs research [7]. To these aims, an ideal scheme is to emphasize these two objectives in parallel.

Biopolymers are naturally abundant and environment friendly polymer alternatives, which are widely used in medical, agricultural and environmental industries due to their especially renewable, sustainable and nontoxic properties when compared to petroleum-based polymers [8]. According to the Food and Agriculture Organization (FAO, QC, Canada), around 35 million tons of natural fibers are harvested each year, which are a fundamental resource that can be used to produce biopolymers [9,10]. In the last decades, various biopolymers, including polysaccharides, proteins and nucleic acid, obtained from animals, plants and microbes, have been employed to packaging materials, drug delivery and regenerative medicine [11,12]. As significant types of biopolymers, natural polysaccharides in particular have some excellent properties owing to their chemical and structural diverse [13,14]. The differences ranging in charge, chain lengths, monosaccharides sequences, and stereochemistry give the highest capacity for the development of advanced functionalized materials and biomedicines [15]. Especially, the hydrophilic groups of polysaccharides can form non-covalent bonds with tissue cells and thus serve in cell–cell recognition and adhesion [16,17]. Moreover, for multi-gene, multi-step devastating disease such as cancer, diabetes and cardiovascular diseases, polysaccharides have a tendency to be more selectively to more than one specific site, eliminating the disadvantages of one-target strategy and preventing the over or under dosing of traditional delivery system [18,19]. Owing to the very safe and stable biodegradation, and biocompatibility, polysaccharides are considered as the most promising hosts in the synthesis of polysaccharide based metallic nanoparticles (PMNPs) with guest metallic ion and MNPs [20,21]. Besides, the host polysaccharides can assemble a carrier with metallic ion and hydrophobic chemical drugs such as doxorubicin, levofloxacin, cefotaxime, ceftriaxone, and ciprofloxacin for targeted drug delivery [22–24]. Polysaccharides can also act as good reducing and stabilizing agents to regulate the physical properties of PMNPs during synthesis process [25]. Over the last decades, remarkable progress has been achieved in the study of PMNPs through host–guest strategy (Figure 1) [26,27]. Therefore, it is necessary to review the recent progresses in PMNPs area.

Although there are several relevant reviews about MNPs, reviews that introduce nanoparticles from the perspective of green synthesis of PMNPs through host–guest strategy are still limited [28]. In this review, a basic introduction of the utilization of natural polysaccharides as guest molecules, conjugated with the host molecules metal ions or MNPs to form PMNPs is given. First, we provide an in-depth introduction on the two common synthesis approaches and characterization methods. Then, the applications of PMNPs in different fields are summarized and discussed in detail. Finally, the potential toxic risks are demonstrated with both in vitro and in vivo evaluation, and future perspectives are presented. Patented PMNPs are not discussed in this review.

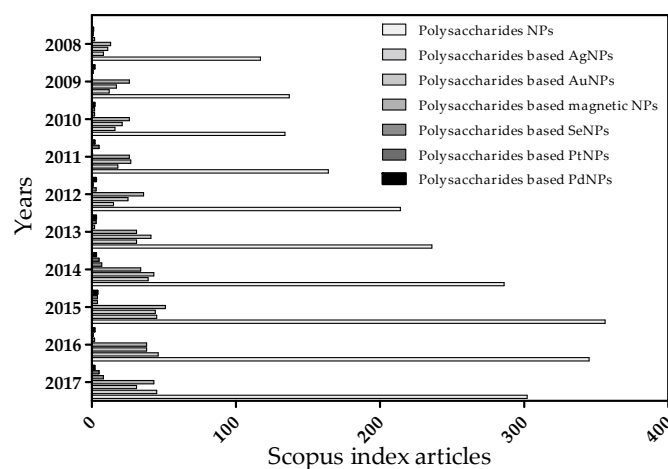


**Figure 1.** Scopus-indexed articles for polysaccharide based nanoparticles (NPs) and metallic nanoparticles (MNPs). (Archived until 6 November 2017).

## 2. Preparation of PMNPs

It is widely accepted that the size, structure and corresponding physical, chemical and biological properties of nanoparticles are largely dependent on the preparation method [29]. Therefore, the selection of synthesis approach is crucial in achieving the appropriate properties of nanoparticles [30]. Generally, nanoparticles are prepared through a variety of chemical and physical methods, which bring serious problems such as high energy consumption, use of large amount of toxic solvents, and generation of hazardous byproducts [31]. Moreover, nanoparticles synthesized from chemical approach are not suitable in biomedical applications owing to the presence of toxic capping agents [32]. Alternatively, developing green synthesis approaches that use mild reaction conditions and non-toxic reaction precursors can eliminate the drawbacks of conventional approaches [33].

Green synthesis of MNPs, using natural polysaccharides as stabilizing and reducing agents, are considered to be a promising area in nanotechnology [34]. Currently, two approaches are involved in the green synthesis of nanoparticles: top-down and bottom-up approaches (Figure 2) [35]. In top-down synthesis, the suitable starting materials are reduced in size using physical treatments such as mechanical milling, thermal ablation or chemical treatment such as chemical etching [36]. After preliminary treatment, the surface of the MNPs will be altered and the high temperature and pressure during the size reduction may induce the oxidation of the nanoparticles, which can affect their physical properties and surface chemistry [35]. Therefore, bottom-up synthesis (self-assembly) is the most frequently chosen approach in the preparation of PMNPs. In a typical bottom-up synthesis, a metallic precursor is either decomposed or reduced to zero-valent state to form the building blocks (smaller entities), followed by the nucleation and nanocrystals growth [37–39]. During this process, polysaccharides can act as the hosts to combine with guest metallic ions and MNPs through noncovalent bonding, and then the order of free energy is altered to realize the stabilization, morphological control and kinetic growth of the MNPs [40]. In addition, the stereogenic centers of polysaccharides will also benefit for the anchoring of the MNPs [1]. In contrast to the harsh reaction condition of top-down approach, the bottom-up synthesis process can occur in the bulk solution or in droplets, which is easy to regulate through controlling the process conditions [41]. Therefore, PMNPs, synthesized through bottom-up synthesis approach that involved in host–guest strategy, are relatively homogeneous compared to those synthesized through top-down approach.

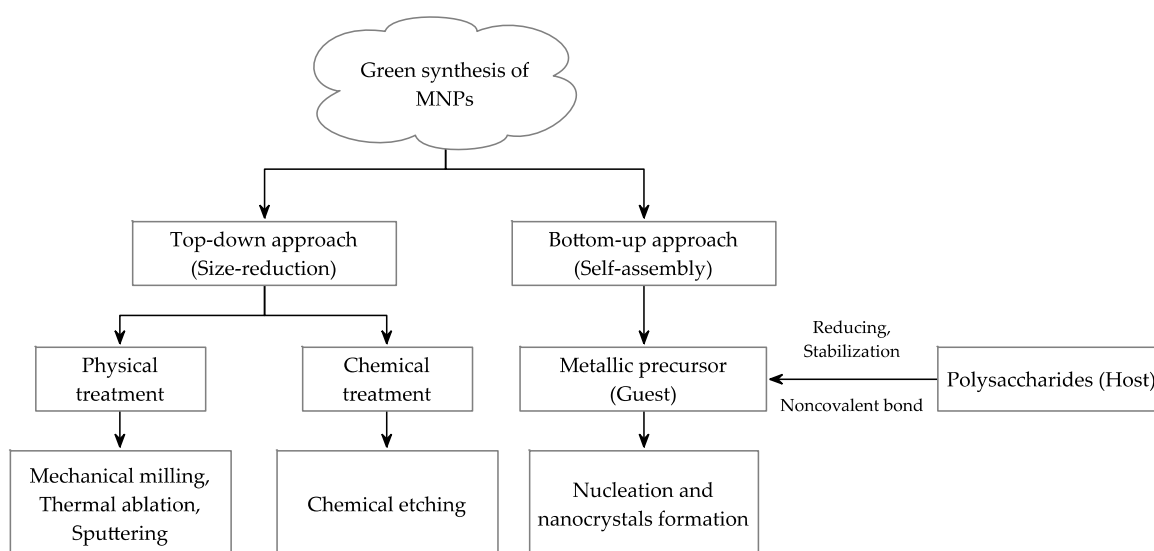


**Figure 2.** Overall approaches for the synthesis of PMNPs.

Although PMNPs with different properties were achieved by regulating the temperature, reaction time and different molar ratios of polysaccharides and metal ions in most studies, there are some attempts that try improving the efficiency in the preparation of PMNPs [42]. The application of microwave heating in the synthesis of sulfated chitosan coated AuNPs resulted in a lower Gibb's free

energy and thus stimulated the activation of reaction [43,44]. Radiolytic reduction was also proven to be helpful in the nucleation, growth and aggregation of PMNPs during the synthesis process [45]. Owing to the different charges of metallic ions and polysaccharides in the solution, electrochemical synthetic techniques were considered to have great potential in the regulation of PMNPs synthesis. In addition, other techniques that could control the synthesis of PMNPs such as microemulsion and photoinduced reduction also need to be attempted in further study [46].

### 3. Characterization of PMNPs

Nanoparticles are of great scientific interests as they combine bulk materials and atomic or molecular structures together [35]. These unique properties are largely associated with their physical characteristics such as diameter, molar volume, morphology and dispersibility [31]. Usually, nanoparticles have a spherical structure [47]. As for sophisticated nanoparticles, core-shell structure and particle distribution are also attractive for specific applications [48]. Thus, many techniques have been explored to elucidate the structure and spectroscopic characters of PMNPs in the literature (Figure 3).

As the basic parameter of nanoparticles, size and morphology are firstly considered in many studies. Scanning electron microscopy (SEM) can give the information about the size, distribution and the shape of the nanoparticles [49]. However, the drying and contrasting process will alter the characteristics of nanoparticles, leading to imaging faults or artifacts [50]. Therefore, transmission electron microscopy (TEM) is introduced in the characterization of nanoparticles. It can be used to determine the particle size, dispersion and aggregation in aqueous environment with a high spatial resolution ( $<1.0$  nm, Figure 3E) [51]. In addition, TEM can provide more details at the atomic scale such as crystal structure, which is more powerful and competitive than SEM [52]. However, many PMNPs are irregular in shape and thus hard to define. Moreover, they also tend to form large particles, and it is hard to attribute the reason to polydispersity or agglomeration [53]. In addition, it is difficult to measure the relevant size of some metallic colloids attached to drugs by TEM physiologically [49]. One technique that can solve this problem is dynamic light scattering (DLS), which can provide a measurement of particle size in solution [54]. In a DLS measurement, the nanoparticles will cause the fluctuations of the laser light intensity, which is recorded and used to determine the equivalent sphere hydrodynamic diameter of the particles [55]. DLS is also sensitive to flexible biological molecules, such as proteins and polysaccharides and thus suitable for the characterization of PMNPs [52]. Nevertheless, owing to the electron dispersion mechanism of DLS, it cannot provide information about the particle with heterogeneous size distributions [56]. Nanoparticles with similar sized distribution are also not well separated from each other in DLS measurement. Considering the diversity and ambiguity of nanoparticles, multiple techniques are commonly used to investigate nanoparticles size such as the combination of TEM and DLS [49].

UV-visible spectroscopy plays a significant role in the illustration of optical properties of PMNPs. It can monitor the quantitative formation and provide information for the size measurement of nanoparticles through different response to the electromagnetic waves, ranging from 190.0 nm to 700.0 nm [57]. The effects of concentration and pH on the stability and aggregation state of PMNPs in different time can also be recorded by UV-visible spectroscopy [35]. Fourier-transform infrared spectroscopy (FTIR) is basically applied to elucidate the functional groups from the spectrum. It can provide information about capping and stabilization of PMNPs, and therefore is utilized to demonstrate the conjugation between MNPs and polysaccharides [58]. X-ray diffraction (XRD) is the primary tool for the determination of the crystal property of PMNPs such as crystallite size and lattice strain [59]. Typically, XRD is useful for the characterization of the size and shape of crystalline PMNPs at the atomic scale. However, the requirement of single conformation and high atomic numbers of crystals limits the application of XRD [60]. In contrast to XRD, small-angle X-ray scattering (SAXS) can provide the information of the crystalline and amorphous PMNPs [51]. By analyzing the intensity of the X-ray, the size distribution, shape, orientation and structure of the nanoparticles can be well illustrated [61]. On the other hand, SAXS can give a holistic characteristic of the PMNPs, which is more effective than XRD. Nevertheless, the crystallite size of the PMNPs is

not exactly the same as the particle size due to the polycrystalline aggregates of nanoparticles [62] and the lattice strain can provide detailed information about the distribution of lattice constant arising from crystal imperfections [63]. As for magnetic nanoparticles, a superconducting quantum interference device (SQUID) magnetometer is introduced to investigate their magnetization property, offering great insights into their application in specific field [64].

In addition to the above techniques, the number of novel methods for the characterization of PMNPs, such as scanning tunneling microscopy (STM), atomic-force microscopy (AFM), Raman scattering and electron spin resonance (ESR) spectroscopy, is growing rapidly, providing more evidence for their applications [35].

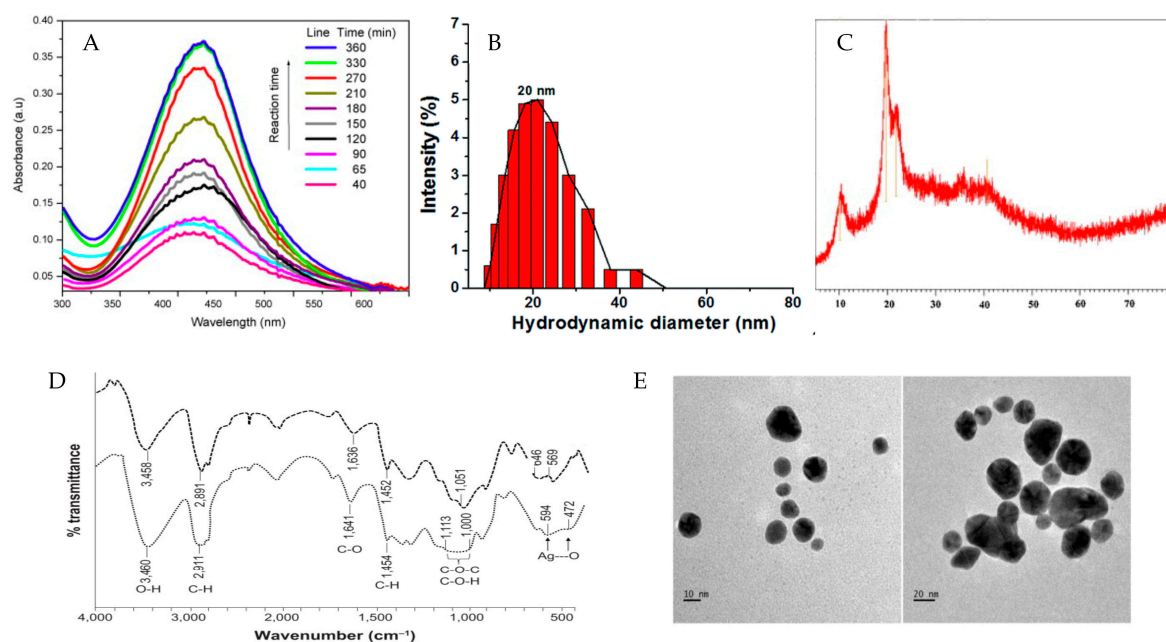


**Figure 3.** Overall scheme for the illustration of different methods to characterize PMNPs: (A) UV-vis spectra of AgNPs; (B) particle size distribution of AgNPs analyzed by DLS; (C) X-ray diffraction spectra of ZnSNPs; (D) FTIR spectra of AgNPs; and (E) TEM images of AuNPs. Reproduced with permission [23,43,65–67].

#### 4. Application of PMNPs

Polysaccharide-based metallic nanoparticles have been extensively used in numerous technological fields owing to their remarkable physical, chemical and biological properties. Herein, the applications of PMNPs are introduced, specifically in wound healing, targeted delivery, biosensing, catalysis and agents with antimicrobial, antiviral and anticancer capabilities.

##### 4.1. Antimicrobial and Antiviral Property of PMNPs

Microbial infections are responsible for most common clinical diseases worldwide, bringing big threats to human public health [68]. Currently, the antimicrobial agents in the market are quaternary ammonium salt, metal salt solutions and antibiotics [33]. Unfortunately, the poor effectiveness and overuse of these agents have led to growing drug resistance of pathogenic bacterial and fungi strains, especially multidrug resistance strains [69]. Infections caused by these strains are more difficult to cure and prevent. Therefore, it is urgent to find novel antimicrobial agents with low toxicity and high efficiency or alternative therapies to solve these problems. Among all the candidates used for the treatment of bacterial infections, MNPs, especially AgNPs, have drawn much attention due to their small size, large surface to volume ratio and tunable plasmon resonance characteristics [70,71]. Since the 1920s, AgNPs were officially approved by the FDA administration to be used in wound therapy as an antibacterial agent; the exploration of MNPs in antibacterial field has increased rapidly [72].

Nowadays, numerous kinds of PMNPs have been synthesized and demonstrated to have significant antimicrobial potential (Table 1). Various methods had been applied to evaluate the antimicrobial activity of PMNPs (Figure 4). Among the methods, agar well diffusion method is the most widely used one to assess the antimicrobial activities of PMNPs against different bacteria and fungi due to its easy, quick and intuitive properties (Figure 4A). Results showed that AgNPs stabilized by different polysaccharides have effective antimicrobial effects on both Gram-positive bacteria, such as *S. epidermidis*, *S. aureus*, *S. lutea*, *B. subtilis*, *L. fermentum*, *E. faecium*, *B. licheniformis*, *B. cereus*, *K. rhizophila*, *S. pyogenes*, *Actinomycetes*, *Staphylococcus*, *S. pneumoniae*, *L. monocytogenes*, and *E. faecalis*, and Gram-negative bacteria, such as *E. coli*, *P. aeruginosa*, *K. planticola*, *K. pneumoniae*, *V. parahaemolyticus*, *P. vulgaris*, *S. typhimurium*, *A. hydrophila*, and *V. cholerae*. In addition, they also exhibited an extensively antifungal activity against *C. albicans*, *F. oxysporum*, *A. niger*, *T. rubrum*, *C. krusei*, and *A. flavus*. It appeared that different kinds of strains had different sensitivities toward polysaccharide-based AgNPs. Gram-negative bacteria were more likely to be affected due to their membrane compositions and the negatively charged cell wall, which made it easier to attach the released  $\text{Ag}^+$ , which resulted in cell death [69]. Gram-positive bacteria were less susceptible to  $\text{Ag}^+$  compared to Gram-negative bacteria [33]. Confocal laser scanning microscopy (CLSM) was another method that used to assess the antimicrobial activities of polysaccharide-based AgNPs by measuring the fluorescence intensity of cells (Figure 4B) [73]. Besides, light microscopy could show the reduced biofilm on the glass surface and SEM could observe the changes in the shape and appearance of bacteria cells, providing more straightforward visualization choices (Figure 4C,E) [44,74]. It has been reported that the binding of  $\text{Ag}^+$  to oligonucleotides would cause changes in the fluorescence excitation and emission spectrum [72]. Thus, 3D fluorescence spectroscopy was introduced to investigate the interaction between  $\text{Ag}^+$  and DNA of bacteria (Figure 4D). Furthermore, minimum inhibitory concentration (MIC) is widely applied to evaluate the antimicrobial activity of PMNPs against bacteria and fungi that cultured in liquid medium [23].

Regardless of the fact that most reported PMNPs with antimicrobial activity were AgNPs, there are other PMNPs that exhibited great antimicrobial potential. AuNPs stabilized by bacterial exopolysaccharides and sulfate chitosan exhibited excellent antimicrobial properties, as assessed by the approaches of MIC, agar plate and SEM [25,75,76]. Polysaccharide-based SeNPs showed effective inhibitory activity on the growth of both bacteria and fungi in the agar plate [39]. In addition, starch capped CuNPs were also demonstrated with antimicrobial capability [77]. Nevertheless, the mechanisms underlying the antimicrobial effects of PMNPs remained unclear. Other proposed mechanisms such as interaction with enzymes and DNA, free radical production should be given more concern [33].

**Table 1.** Summary of literature data regarding the antimicrobial property of PMNPs.

| Resource  | Polysaccharides                   | Metals                            | Diameter (nm) | Shape                         | Antimicrobial strains  | References |
|---|-----------------------------------|-----------------------------------|---------------|-------------------------------|--|------------|
| <i>Lactobacillus plantarum</i>  | Exopolysaccharides                | Au                                | 10.0–20.0     | Spherical/ellipsoidal         | <i>E. coli</i> , <i>S. aureus</i> , <i>K. pneumoniae</i>   | [25]       |
| <i>Pleurotus tuber-regium</i>   | Polysaccharides-protein complexes | Se                                | 122.0         | -                             | <i>Staphylococcus</i> , <i>T. rubrum</i>   | [39]       |
| -   | Hydroxypropylcellulose            | Ag                                | 25.0–55.0     | Spherical                     | <i>E. coli</i> , <i>B. subtilis</i> , <i>S. aureus</i> , <i>P. aeruginosa</i> , <i>S. epidermidis</i> , <i>A. niger</i> , <i>Actinomycetes</i>   | [43]       |
| -   | 6-O-chitosan sulfate              | Au                                | 15.0          | Spherical                     | <i>E. coli</i>   | [44]       |
| Tamarind  | Carboxymethyl polysaccharides     | Ag                                | 20.0–40.0     | Spherical/polygonal           | <i>E. coli</i> , <i>B. subtilis</i> , <i>S. typhimurium</i>  | [54]       |
| -   | Agarose/dextran/gelatin           | Fe <sub>2</sub> O <sub>3</sub>    | 10.0          | Dumbbell shape                | <i>S. aureus</i> , <i>A. hydrophila</i> , <i>S. pyogenes</i> , <i>P. aeruginosa</i>  | [64]       |
| -   | Guar gum                          | Ag                                | 16.0          | Spherical                     | <i>B. subtilis</i>   | [65]       |
| -   | Chitosan-g-poly(acrylamide)       | ZnS                               | 19.0–26.0     | Triangular                    | <i>E. coli</i>   | [66]       |
| <i>Astragalus membranaceus</i> root   | Crude polysaccharides             | Ag                                | 65.1          | Spherical                     | <i>S. aureus</i> , <i>E. coli</i> , <i>S. epidermidis</i> , <i>P. aeruginosa</i>   | [69]       |
| -   | Pullulan                          | Ag                                | 2.0–30.0      | Spherical/oval-shaped         | <i>E. coli</i> , <i>K. pneumoniae</i> , <i>L. monocytogenes</i> , <i>P. aeruginosa</i> , <i>Aspergillus spp.</i> , <i>Penicillium spp.</i>   | [70]       |
| -   | Pectin                            | Ag                                | 5.4–10.6      | Spherical                     | <i>E. coli</i> , <i>S. epidermidis</i>   | [73]       |
| -   | Chitosan                          | Ag/ZnO                            | 10.0–65.0     | Spherical/Uneven distribution | <i>E. coli</i> , <i>P. aeruginosa</i> , <i>L. fermentum</i> , <i>E. faecium</i> , <i>S. aureus</i> , <i>B. licheniformis</i> , <i>B. subtilis</i> , <i>B. cereus</i> , <i>V. parahaemolyticus</i> , <i>P. vulgaris</i> | [23,74]    |
| <i>Bacillus megaterium</i>  | Exopolysaccharides                | Au                                | 5.0–20.0      | Spherical                     | <i>E. coli</i> , <i>B. cereus</i> , <i>S. aureus</i> , <i>S. epidermidis</i> , <i>K. pneumoniae</i> , <i>S. typhi</i> , <i>P. aeruginosa</i> , <i>V. cholerae</i> , <i>S. pneumoniae</i>                               | [75]       |
| Seaweed<br><i>Chondracanthuschamissoi</i> ,<br><i>LessoniaSpicata</i> , <i>Ulvasp</i> | Polysaccharides                   | Ag/Au                             | 10.0/25.0     | Spherical                     | <i>P. aeruginosa</i> , <i>S. typhimurium</i>   | [76]       |
| -   | Starch                            | Cu(NO <sub>3</sub> ) <sub>2</sub> | 5.0–12.0      | Spherical                     | <i>E. coli</i> , <i>S. aureus</i> , <i>Salmonella typhi</i>  | [77]       |

|  |                                  |    |           |                            |   |            |
|--|----------------------------------|----|-----------|----------------------------|---|------------|
| <i>Padina tetrastromatica</i>  | Fucoidan                         | Ag | 17.0      | Spherical                  | <i>B. subtilis</i> , <i>Bacillus</i> sp. <i>K. planticola</i> , <i>K. pneumoniae</i> , <i>S. nematodiphila</i> , <i>Streptococcus</i> sp. | [78]       |
| -  | $\beta$ -glucan                  | Ag | 15.0      | -                          | <i>E. coli</i> , <i>Methylobacterium</i> spp., <i>Sphingomonas</i> spp.   | [79]       |
| <i>Arthrobacter</i> sp. B4   | Exopolysaccharides               | Ag | 9.0–72.0  | Face-centred-cubic         | <i>P. aeruginosa</i> , <i>S. aureus</i> , <i>C. albicans</i> , <i>F. oxysporum</i>  | [80]       |
| <i>Cordyceps sinensis</i> (Berk.)  | Exopolysaccharides               | Ag | 50.0      | Spherical                  | <i>E. coli</i> , <i>S. aureus</i>   | [81]       |
| -  | Xanthan gum/chitosan             | Ag | 5.0–20.0  | Spherical                  | <i>E. coli</i> , <i>S. aureus</i>   | [22,82,83] |
| -  | Chitosan-carboxymethyl cellulose | Ag | 5.0–20.0  | Irregular shape            | <i>E. coli</i> , <i>S. aureus</i> , <i>P. aeruginosa</i>  | [84]       |
| <i>Bradyrhizobium japonicum</i> 36   | Exopolysaccharides               | Ag | 5.0–50.0  | Rod/oval-shaped structures | <i>E. coli</i> , <i>S. aureus</i>   | [85]       |
| <i>Klebsiella oxytoca</i>  | Exopolysaccharides               | Ag | 6.0–16.0  | Spherical                  | <i>E. coli</i> , <i>K. rhizophila</i>   | [86]       |
| <i>Lentinus squarrosulus</i> (Mont.)   | Hetero polysaccharides           | Ag | 1.3–4.5   | Spherical                  | <i>E. coli</i>  | [87]       |
| <i>Pleurotus florida</i>   | Glucan                           | Ag | 1.3–2.5   | Spherical                  | <i>K. pneumoniae</i>  | [88]       |
| Lactic acid bacterium  | Exopolysaccharides               | Ag | 2.0–15.0  | Spherical/triangular       | <i>E. coli</i> , <i>K. pneumoniae</i> , <i>L. monocytogenes</i> , <i>P. aeruginosa</i>  | [89]       |
| -  | Dextran/sucrose                  | Fe | 5.8/7.3   | Spherical                  | <i>E. coli</i> , <i>P. aeruginosa</i> , <i>E. faecalis</i> , <i>C. krusei</i>   | [90]       |
| -  | Mesoporous starch                | Ag | 5.0–25.0  | Spherical                  | <i>E. coli</i> , <i>S. aureus</i>   | [91]       |
| <i>Anogeissus latifolia</i>  | Gum ghatti                       | Ag | 5.5–5.9   | Uneven shape               | <i>E. coli</i> , <i>S. aureus</i> , <i>P. aeruginosa</i>  | [92]       |
| Marine macro algae<br>( <i>U. fasciata</i> , <i>P. capillatae</i> ,<br><i>J. rubins</i> , <i>C. sinusa</i> ) | Polysaccharides                  | Ag | 7.0–20.0  | Spherical                  | <i>E. coli</i> , <i>S. aureus</i>   | [93]       |
| <i>Bacillus subtilis</i>   | Exopolysaccharides               | Ag | 1.1–6.7   | Spherical                  | <i>S. aureus</i> , <i>P. aeruginosa</i>   | [94]       |
| <i>Cochlospermum gossypium</i>   | Gum kondagogu                    | Ag | 18.9–55.0 | Spherical                  | <i>E. coli</i> , <i>S. aureus</i> , <i>P. aeruginosa</i>  | [95]       |
| <i>Porphyra vietnamensis</i>   | Sulfated polysaccharides         | Ag | 10.0–16.0 | Spherical                  | <i>E. coli</i> , <i>S. aureus</i>   | [96]       |
| <i>Portulaca</i>   | Arabinogalactan                  | Ag | 20.0–35.0 | Spherical                  | <i>C. albicans</i> , <i>S. cerevisiae</i> , <i>A. niger</i> ,<br><i>A. flavus</i>   | [97]       |



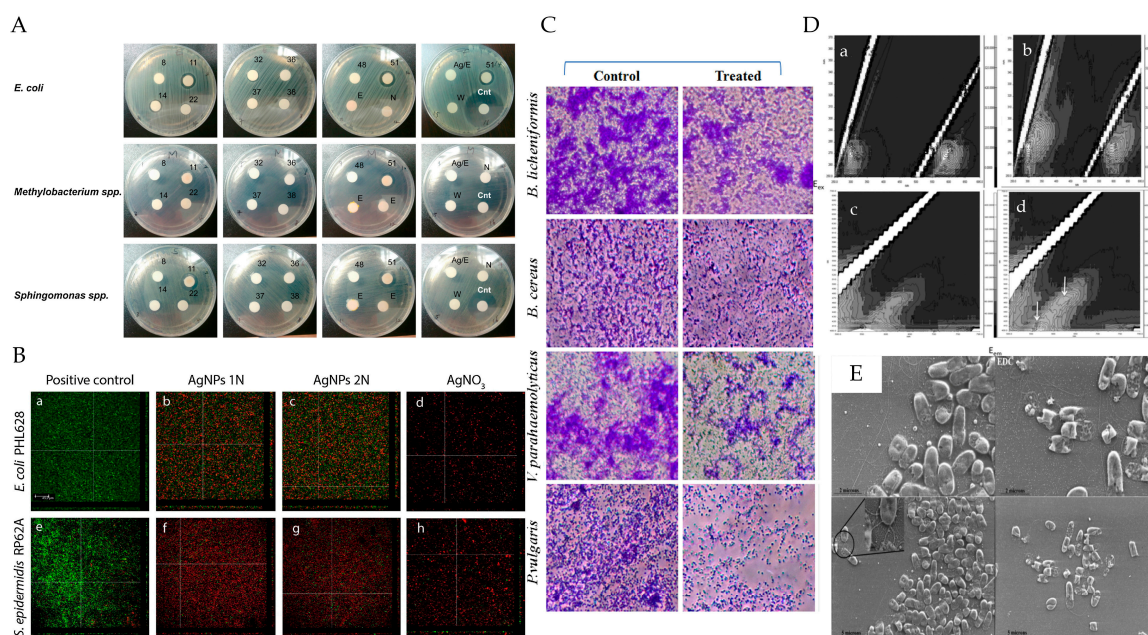


**Figure 4.** Overall scheme for the illustration of different methods to evaluate the antimicrobial activity of PMNPs: (A) antimicrobial tests on agar plate; (B) CLSM images of bacterial treated with p-AgNPs; (C) light microscopy images of bacterial treated with CS/Ag/ZnO nanocomposite; (D) fluorescent fingerprints of DNA of *E. coli* in the presence of exopolysaccharides based AgNPs; and (E) SEM images of bacterial treated with S-Chi@Au. Reproduced with permission [44,73,74,79,96].

In the last decades, viruses have become serious concerns due to their dramatic breakout worldwide, including the human immunodeficiency virus (HIV), influenza virus, Zika virus and severe acute respiratory syndrome virus (SARS). The infection of virus has brought unprecedented crisis for public health, leading to a staggering societal cost [98]. Unlike the pathogenic microorganisms, viruses are infectious agents that replicate only in living cells, which can be eliminated by antibodies produced by the immune system instead of antibiotics [99]. The viral diversity and rapid mutability properties make the diagnosis and prevention of viruses especially difficult in the clinic [100]. PMNPs have posed various unique advantages, which make them attractive in solving the virus problems. It had been reported that tailored glycan functionalized AuNPs (13.0 nm) could bind with the influenza viruses (vieH5N1, shaH1N1 and H7N9) and form an aggregation on the surface of virus, resulting in a discriminable plasmon band shift and color change subsequently [100,101]. The polysaccharide-capped AgNPs (15.0 nm) were demonstrated to absorb and quench dye-labeled single-stranded DNA, which could be utilized as an effective fluorescence sensing platform for human immunodeficiency virus (HIV) [102]. In addition, polysaccharide-coated AgNPs (10.0 nm, 25.0 nm) were also illustrated to inhibit the viral replication and reduce the progeny production of Tacaribe virus and Monkeypox virus [103,104]. Nevertheless, the antiviral mechanism of polysaccharide-based MNPs is still unclear [105]. It is critical to understand the precise interactions between nanoparticles and virus, especially their influences on the binding of virus to host receptors, in further research.

#### 4.2. Anticancer Property of PMNPs

Cancer is a dominant factor of morbidity and mortality globally [106]. It has been estimated that about 90.5 million people are diagnosed with cancer, and the tendency is continually rising despite the preventive measures and therapeutic efforts in the past decades [107]. Recently, PMNPs, used in nanomedicine, provide an alternative opportunity in the prevention, diagnosis and treatment of cancer. Its sophisticated targeting strategies and multi-functional characters have remarkable advantages in the improvement of pharmacokinetics and pharmacodynamics profiles compared to

conventional therapeutics [108]. Therefore, the application of PMNPs in cancer treatment as nanomedicine has emerged as a fruitful area in nanotechnology and extensive investigations have addressed this issue (Table 2).

3-(4,5-dimethylthiazol-2-yl)-2,5-diphenyltetrazolium bromide (MTT) assay is the most commonly used method to assess the effects of different toxicants on the viability of cells [109]. Pectin mediated AuPNs showed an obvious cytotoxicity on human breast adenocarcinoma cells MCF-7 and MDA-MB-231 with the concentration of 10  $\mu\text{g/mL}$  via MTT reduction capability evaluation. Meanwhile, DNA of the cancer cells was also significantly fragmented indicating potential anticancer activity [110]. The noticeable alterations in the cellular shape and morphology were recognized as another hallmark of apoptosis of cancer cells [111]. It has been reported that chitosan based AgNPs (20.0 nm) reduced the viability of human lung adenocarcinoma cells A549/Lu, human hepatocellular carcinoma cells HepG2, human epidermic carcinoma cells KB and human breast carcinoma cells MCF-7 by reducing cell density and inducing the shrinkage and blebbing of the cells [23,112]. SeNPs have received additional attention in the prevention of cancers. Accumulated evidence illustrated that they could stimulate the immune system, modulate thioredoxin reductase activity, maintain cell redox balance and induce apoptosis of cancer cells [113]. D-glucose based SeNPs have been proven to exert anticancer activity against HepG2 cells at the cell cycle of S phase (Figure 5) [114]. In addition, absorption of polysaccharide-based SeNPs could also result in reactive oxygen species (ROS)-induced apoptosis of cancer cells through mitochondria mediated pathway [111].

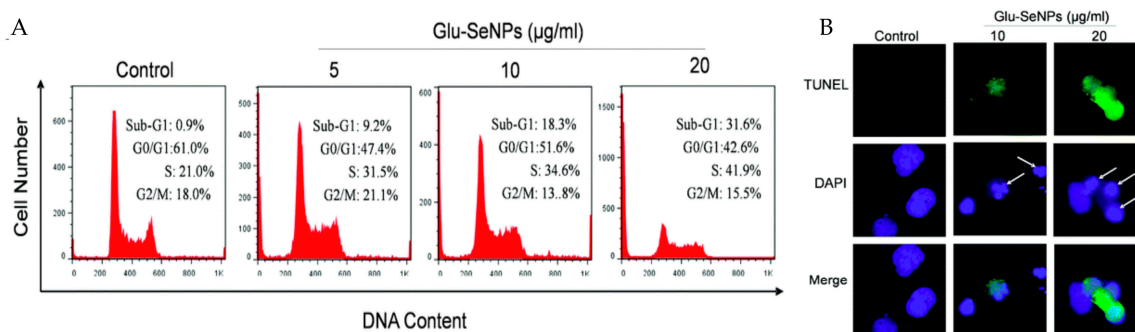


**Figure 5.** Apoptosis induced by Glu-SeNPs in cancer cells: **(A)** flow cytometric analysis of cancers cells; and **(B)** DNA fragmentation and nuclear condensation. Reproduced with permission [114].

Caspases-3 activation is another factor that involved in the execution phase of apoptosis [115]. Results showed that polysaccharide-based SeNPs and iron oxide NPs could significantly increase the activity of caspases-3 in a dose-dependent manner, resulting in the death of cancer cells [116,117]. Despite these results in the prevention of cancer cells, polysaccharide-based AuNPs were green synthesized to sufficiently eradicate tumors by means of heat and photothermal therapy [118,119]. In addition, the inhibition of *Tamarindus indica* polysaccharide-based AuNPs on tumor growth was also achieved by stimulating the proliferation of lymphocyte cells in vivo [111]. Therefore, PMNPs were good therapeutical agents to assist the cancer treatment.

**Table 2.** Summary of literature data regarding the anticancer property of PMNPs.

| Resource                                  | Polysaccharides                   | Metals                         | Diameter (nm) | Shape           | Cancer types   | References |
|---|-----------------------------------|--------------------------------|---------------|-----------------|--|------------|
| <i>Tamarindus indica</i>                  | Galactoxyloglucan polysaccharides | Au                             | 20.0          | Spherical       | Murine cancer cells (DLA, EAC)                       | [109]      |
| <i>Musa paradisiaca/Ganoderma lucidum</i> | Pectin                            | Au                             | 8.0           | Spherical       | Human breast adenocarcinoma cells (MCF-7/MDA-MB-231) | [110]      |
| <i>Tamarindus indica</i>                  | Polysaccharides PST001            | Au                             | 15.0–20.0     | Circular        | Breast cancer cells (MCF7), Leukemia cells (K562)    | [111]      |
| -   | Fucoidan-mimetic glycopolymer     | Au                             | 20.0–55.0     | Spherical       | Human colon cancer cells (HCT116)                    | [112]      |
| <i>Sargassum muticum</i>                  | Aqueous extract                   | Fe <sub>3</sub> O <sub>4</sub> | -             | -               | HepG2, MCF-7, HeLa, Jurkat                           | [116]      |
| <i>Polyporus rhinocerus</i>               | Polysaccharide–protein complexes  | Se                             | 50.0          | Spherical       | Human lung adenocarcinoma cells (A549)               | [117]      |
| <i>Halomonas maura</i>                    | Sulfated exopolysaccharides       | Au                             | 70.0–107.0    | Quasi-spherical | Breast cancer cells (MCF7)<br>Glioma cells (GI-1)    | [118]      |
| -   | Gum arabic                        | Au                             | 0.9–2.3       | Spherical       | Human breast adenocarcinoma cells (MDA-MB-231)       | [119]      |
| <i>Leuconostoc spp.</i>                   | Dextran                           | Au                             | 49.0          | Spherical       | Ehrlich ascites carcinoma (in vivo)                  | [120]      |
| -   | Chitosan                          | Ag                             | 5.0–15.0      | Spherical       | A549, HepG2, Lu, KB, MCF-7                           | [23,121]   |
| <i>Chlorella vulgaris</i> LARG-3          | Polysaccharides                   | Pt                             | 18.0–38.0     | Quasi-spherical | Ovarian cancer A2780                                 | [122]      |
| <i>Lentinus edodes</i>                    | Lentinan                          | Se                             | 28.0          | Spherical       | Human cervix carcinoma cells (HeLa)                  | [123]      |
| -   | Hyaluronic acid                   | Se                             | 66.8          | Spherical       | Heps solid tumor (in vivo)                           | [124]      |
| <i>Undaria pinnatifida</i>                | Polysaccharides                   | Se                             | 59.0          | Spherical       | Human melanoma cells (A375)                          | [125]      |
| <i>Spirulina</i>                          | Polysaccharides                   | Se                             | 20.0–50.0     | Spherical       | Human melanoma cells (A375)                          | [126]      |
| <i>Pleurotus tuber-regium</i>             | Polysaccharide–protein complexes  | Se                             | 44.0–220.0    | Spherical       | Human breast carcinoma (MCF-7)                       | [127]      |

### 4.3. Wound Healing Property of PMNPs

Wound healing is a complex physiological process that follows three overlapping phases including inflammation and tissue remodeling, the rate of which is affected by the type, size and depth of the wound, and especially the presence of bacterial infection [128]. Consequently, conditions that are unfavorable for the colonization of pathogenic bacteria and fungus or helpful for the host repair mechanisms are required to facilitate wound healing progress [129]. Traditional dressings (gauze and tulle) achieve their capability of healing wound by forming a barrier from the external microorganisms and maintain the dry environment of the wound instead of influencing the healing process directly [130]. PMNPs had been extensively proved with excellent antimicrobial activity, providing great potential in the healing of wounds.

Nowadays, several PMNPs had been reported to be suitable for wound management. Pectin (8.0 nm) and chitosan (40.5 nm) coated AgNPs exerted great antibacterial activity on *E. coli* (Gram-negative) and *S. epidermidis* (Gram-positive) both on planktonic and biofilm formation conditions despite the low free Ag<sup>+</sup> concentration [73,129]. It also exhibited cytocompatibility and capability in promoting fibroblasts proliferation through cytokine regulation [131]. Mannan sulfate AgNPs (20.0 nm) were reported to exhibit an enhanced cytocompatibility and promotion in the cellular uptake of murine macrophages, human skin fibroblasts and human keratinocytes. The excision and incision wound models in vivo also showed its repairs in wound area, wound contraction and epithelization period, suggesting promising potential for site-specific wound therapy [132]. In addition, xanthan based film incorporated with AgNPs could stimulate angiogenesis, which was the key factor of granulation tissue regeneration [133]. Nevertheless, more metallic nanoparticles preferred to use hydrogel as their reducing agents, which could be easily removed from the wound site, avoiding further trauma and facilitating re-epithelialization [134]. Usually, hydrogel mediated AgNPs revealed their wound healing ability through inhibition towards microorganisms [22,135,136]. Glucuronoxylan mediated AgNPs (9.3 nm) were proven to promote collagen content, which could stimulate the following re-epithelialization and granulation tissue formation (Figure 6) [137]. Recently, a novel bilayer composite was introduced in the wound dressing, which was more efficient than traditional single layer film. The upper layer, composed of chitosan based AgNPs, was designed to prevent bacterial penetration and ensured the permeability of oxygen to the wound site, while the lower layer, composed of cross-linked chitosan, was designed to improve cell proliferation activity [138]. This bilayer strategy had combined the advantages of both layers, which was an ideal strategy for the investigations of MNP subsequently.

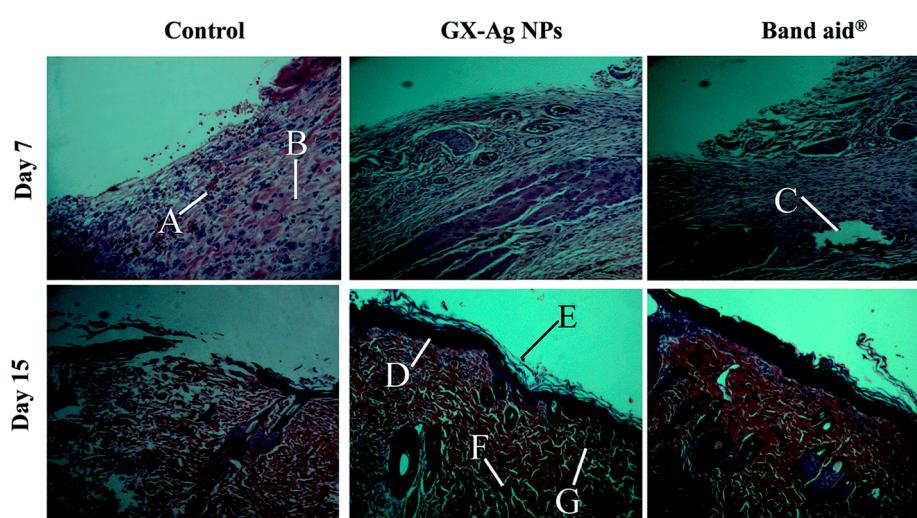


**Figure 6.** Histological examination in wound healing of glucuronoxylan-mediated AgNPs on Day 7, and 15 by Hematoxylin & eosin (H&E) staining: (A) neutrophils accumulation; (B) collagen deposition; (C) hair follicle; (D) epidermis; (E) stratum corneum; (F) dermis; and (G) fibroblasts. Reproduced with permission [137].



#### 4.4. PMNPs in Targeted Delivery

Conventional chemotherapeutic agents have encountered various problems such as high toxicity, large volume of distribution, short lifetime in the body and low solubility, which led to a narrow therapeutic index [107]. Thus, it is critical to develop a directed therapy approaches and increase the efficiency of chemical agents. Nanoparticles represent unique physicochemical characters, which are small enough to traverse most biological membranes and avoid the uptake of the reticuloendothelial system [139,140]. These properties can be easily engineered with regard to the desired gene and drug delivery capacity and controlled release [141]. Over the years, PMNPs exhibited great potential in the targeted drug delivery applications and a summary of the current developments are shown in Table 3.

One common targeted delivery application of PMNPs was to transport the anticancer drugs to the specific sites of cancer cells. It can be observed that the metallic nanoparticles that correspond to anticancer drug delivery are AuNPs, which exhibited a pH dependent release behavior, resulted in a higher release efficiency at pH 5.7 than pH 7.4 [142,143]. Generally, the endosomal pH of cancer cells is acidic, while the endosomal pH of normal cells is neutral [144]. This property will ultimately improve the cytotoxic activity of drugs against cancer cells and reduce their toxicity on normal cells, which is are desirable characteristics for cancer targeted drug delivery [145]. Besides, polysaccharide-based AuNPs revealed desirable optical, electrical and chemical properties, which enabled to display high-amplitude photoacoustic signals in the cancer cells, suggesting promising potential in photoacoustic image-guided drug release and synergistic chemo-photoacoustic therapy [142,146]. Much evidence suggests that there are many receptors on the cell surface, which are responsible for the interaction between PMNPs and the microenvironment around the cells [147]. Based on this knowledge, hyaluronic acid supported AuNPs and *Gracilaria lemaneiformis* polysaccharide-based SeNPs achieved their anticancer effects by recognizing the receptors of CD44 and  $\alpha_v\beta_3$  integrin in specific cancer cells, respectively [147,148], suggesting a new strategy for the design of targeted drug delivery. Another promising site-targeted type of MNPs was magnetic nanoparticles, which could be directed at the specific tissues by means of an external magnetic field and its significance in the anticancer drug delivery had been well discussed in the review [107].

Normally, biological therapeutical agents were susceptible to be hydrolyzed and digested in the gastrointestinal process and their low membrane permeability restricted the potential bioavailability in vivo [149]. Therefore, the possibilities of PMNPs as novel carriers for the delivery of biological agents were exploited. Recently, chitosan reduced AuNPs were demonstrated to enhance the transmucosal delivery of insulin and improve the pharmacodynamic activity [150]. PMNPs also exhibited a safe delivery of DNA in vivo, indicating great potential in gene therapy [151]. Nevertheless, the applications of PMNPs in the delivery of biological agents were still limited and more attempts should be given in this area.

**Table 3.** Summary of literature data regarding the targeted delivery property of PMNPs.

| Resource                              | Polysaccharides  | Metals                         | Diameter (nm) | Shape                 | Targeted delivery   | References |
|---------------------------------------|--|--------------------------------|---------------|-----------------------|---|------------|
| <i>Sphingomonas elodea</i>            | Gellan gum   | Au                             | 12.0–14.0     | Spherical             | Doxorubicin hydrochloride delivery  | [24]       |
| <i>Lactobacillus plantarum</i>        | Exopolysaccharides                                       | Au                             | 20.0–30.0     | Spherical/ellipsoidal | Levofloxacin, cefotaxime, ceftriaxone, ciprofloxacin delivery   | [25]       |
| -                                     | Mannan sulfate   | Ag                             | 17.0–23.0     | Spherical             | Targeting in cellular uptake (J774A.1, TE 353.Sk and HaCaT cells)   | [132]      |
| <i>Fucus vesiculosus</i>              | Fucoidan   | Au                             | 73.0–96.0     | Spherical             | Doxorubicin delivery  | [142]      |
| -                                     | Chitosan-oligosaccharide                                 | Au                             | 58.8–64.8     | Spherical             | Paclitaxel delivery   | [143]      |
| -                                     | $\beta$ -cyclodextrin-hyaluronic acid                    | Au                             | 2.2           | Spherical             | Doxorubicin hydrochloride, paclitaxel, topotecan hydrochloride, camptothecin, irinotecan hydrochloride delivery | [144]      |
| -                                     | Poly(acrylamidoglycolic acid-co-vinylcaprolactam)-pectin | Ag                             | 50.0–100.0    | Spherical             | 5-fluorouracil delivery   | [146]      |
| -                                     | Hyaluronic acid  | Au                             | 50.8–56.0     | -                     | Binding with receptor CD44  | [147]      |
| <i>Gracilaria lemaneiformis</i>       | Polysaccharides  | Se                             | 50.0          | Near-spherical        | $\alpha\beta_3$ integrin receptor mediated endocytosis  | [148]      |
| -                                     | Chitosan   | Au                             | 10.0–50.0     | -                     | Insulin delivery, bioadhesive and intestinal barrier bypass characters  | [150]      |
| <i>Gynostemma pentaphyllum</i> Makino | Folate-conjugated sulfated polysaccharides               | Au                             | 4.0–6.0       | Spherical             | Camptothecin delivery   | [152]      |
| <i>Musa paradisiaca</i>               | Gal-Glc-[Gal-]GlcNAc                                     | Au                             | 1.7–1.9       | Spherical             | Polysaccharides of Targeting in <i>Streptococcus pneumoniae</i> type 14   | [153]      |
| -                                     | $\beta$ -cyclodextrin/chitosan                           | Fe                             | 8.4–16.3      | Spherical             | Prodigiosin delivery  | [154]      |
| -                                     | Gum karaya   | Au                             | 20.0–25.0     | Spherical             | Gemcitabine hydrochloride delivery  | [155]      |
| -                                     | Dextran-lysozyme   | Au                             | 2.5–15.8      | Spherical             | Doxorubicin delivery  | [156]      |
| <i>Saccharomyces cerevisiae</i>       | Mannan   | Fe <sub>3</sub> O <sub>4</sub> | 21.2–48.1     | Ellipsoidal           | Targeting in antigen-presenting cells/macrophage  | [157,158]  |
| -                                     | Starch   | Ag                             | 11.5–19.3     | Spherical             | Targeting in mitochondrial membrane   | [159]      |
| -                                     | k-carrageenan  | Fe <sub>3</sub> O <sub>4</sub> | 4.0           | Spherical             | Methotrexate  | [160]      |

#### 4.5. PMNPs for Biosensing

A biosensor is an analytical device capable of converting a biological event into a physico-chemical signal, which is highly specific and efficient in a low detection limit for the analysis [161]. Nowadays, various biosensors for the detection of chemicals, metal ions, proteins and gas had been reported. PMNPs, had been intensively applied in biosensing field owing to their outstanding optical, electronic and chemical properties [162]. A summary of the current developments in biosensing and probes are shown in Table 4.

Among all the biosensors, optical sensors are the most promising candidates as they are sensitive, flexible and convenient [163]. The basic principles for optic sensors are based on the determination of colorimetric absorbance, reflectance, luminescence, refractive index and light scattering changes [164]. On this basis, some PMNPs had been developed as biosensors and probes. It had been demonstrated that alginate and dextrin based AgNPs showed a concentration dependent changes in the absorbance of manganese (II) and copper (II), separately, suggesting a good application in the detection of metal ions [165,166]. Conventional methods of detection of melamine are complex and time-consuming. Chitosan stabilized AuNPs could lead to a color change in the presence of melamine with the limited concentration of  $6 \times 10^{-6}$  g/L, providing an alternative way for onsite detection of melamine [167]. Ammonia is a toxic pollutant that threatens the health of human [168]. In this regard, ammonia sensors that could detect the ambient ammonia concentrations before damage occurs are necessary. Polysaccharide-based AuNPs and AgNPs had excellent performances in the sensing of ammonia at room temperature with the detection limit of 1 ppb [169,170] and guar gum based AuNPs could present a wider detection range of ammonia from 0.1 parts-per-quadrillion (ppq) to 75,000 parts-per-million (ppm) due to the variations in electrical conductivity [171]. Another toxic pollutant is hydrogen peroxide, which could also be successfully monitored by optic  $\text{H}_2\text{O}_2$  sensor (polysaccharide-based AgNPs) in the concentration range of 0.001 to 10 mM [163]. Tin oxide ( $\text{SnO}_2$ ), commonly known as semiconductor material, exhibited fast response, high sensitivity, low power consumption, mass-produced potency and wide operation working temperature range characteristics, which were especially suitable for the practical applications in gas sensors [172]. Therefore, polysaccharide-based Au-doped  $\text{SnO}_2$  nanoparticles have been bio-green synthesized and their high sensitivity in the sensing of  $\text{NO}_2$  and ethanol vapor make them possible agents for the monitoring of harmful gas [173,174]. In addition, MNPs coated with dextran provided possibilities in the measurement of amino acids and proteins such as cysteine and insulin with high sensitivity [175,176] and other applications in enzyme activity determination and large scale screening were also observed [177,178]. In some situations, fluorescent dyes could be introduced in the synthesis of PMNPs to improve their efficiency and this strategy could be an option for the future development of biosensors [179].

**Table 4.** Summary of literature data regarding the polysaccharide-based MNPs for biosensing.

| Resource                            | Polysaccharides                       | Metals                         | Diameter (nm) | Shape     | Biosensing applications  | References    |
|-------------------------------------|---------------------------------------|--------------------------------|---------------|-----------|--|---------------|
| <i>Ceratonia siliqua</i>            | Locust bean gum                       | Au-SnO <sub>2</sub> /Ag        | 16.0–28.0     | Spherical | Ethanol vapor sensing/hydrogen peroxide sensing                                  | [163,164,174] |
| -                                   | Alginate                              | Ag                             | 10.0–20.0     | Spherical | Detection of manganese (II) ions   | [165]         |
| -                                   | Dextrin                               | Ag                             | 15.0–28.0     | Spherical | Detection of copper (II) ions  | [166]         |
| -                                   | Chitosan                              | Ag/Au                          | 7.3–8.8       | Spherical | Detection of aromatic <i>ortho</i> -trihydroxy phenols/hydrogen sulfide/melamine | [167,180,181] |
| -                                   | Guar gum                              | Au/Pd/Ag                       | 6.0–10.0      | Spherical | Sensor for the detection of ammonia level/electrocatalytic hydrazine             | [169,171,182] |
| <i>Cyamopsis tetragonaloba</i>      | Polysaccharides                       | Au                             | 6.5           | Spherical | Sensor for the detection of ammonia  | [170]         |
| <i>C. arietinum</i> L.              | Water extracts                        | Au-SnO <sub>2</sub>            | 25.0          | Spherical | Sensor for the detection of NO <sub>2</sub>                                      | [173]         |
| <i>Leuconostoc mesenteroides</i> T3 | Dextran                               | Ag/Au                          | 9.9–13.9      | Spherical | Sensor for the detection of cysteine/insulin                                     | [175,176]     |
| -                                   | Cellobiose                            | Au                             | 10.7–33.5     | -         | Measurement of cellobiase activity   | [177]         |
| -                                   | Hyaluronic acid                       | Au                             | 14.0–19.0     | Spherical | Hyaluronidase inhibitor screening  | [178]         |
| Bagasse                             | Xylan                                 | Ag                             | 20.0–35.0     | Spherical | Detection of Hg <sup>2+</sup>  | [183]         |
| -                                   | β-cyclodextrin-dextran-g-stearic acid | Fe <sub>3</sub> O <sub>4</sub> | 59.0–149.0    | Micelles  | Magnetic resonance imaging for monitoring cancer cells                           | [184]         |



#### 4.6. PMNPs in Catalytic Application

Catalysis is an important process that associated with the chemical transformations, which is crucial for the development of modern industry [185]. As the key factors in catalysis, catalysts participate in the chemical reaction in a specific path without itself being consumed and they decide the rates of the reaction [1]. Ideally, catalysts can convert a large quantity of reactants, while consume less materials under mild reactive conditions [186]. However, traditional catalysts usually produce unwanted byproducts which have significant impacts on the environment [187]. In this regard, homogeneous catalysts that exhibited high selectivity had received much more attention. Among all the nanocatalysts, PMNPs are especially attractive due to their high surface area to volume ratios and high surface energy, which allowed their catalytic sites to be accessible [188]. Since catalytic reactions required transition metals, polysaccharides could provide a suitable functional support for dispersing the noble MNPs as hosts and make the size and shape of catalysts more controllable [1]. Thus, various studies had highlighted the possibilities of PMNPs in catalytic application (Table 5) and the reaction mechanisms were shown in Figure 7.

4-nitrophenol (4-NP) is a phenolic compound that widely exists in the wastewater [189]. It can cause serious damages to the central nervous system, kidney and liver in both animals and human beings [190]. Thus, various methods had been developed to reduce 4-NP to 4-aminophenol (4-AP), which was a common intermediate in the manufacture of antipyretic and analgesic drugs that friendly to the environment [191]. Commonly, the reduction of 4-NP to 4-AP was achieved in the presence of appropriate reducing agent named  $\text{NaBH}_4$  and the reaction could be monitored by UV-visible spectroscopy [192]. Thus, this model evaluation system was used to determine the catalytic activity of PMNPs. Nowadays, AgNPs and AuNPs stabilized by different kinds of polysaccharides were the most effective nano catalysts that reported to involve the conversion of 4-NP. *Cordyceps sinensis* exopolysaccharide-based AgNPs (5.0 nm) showed a good capability in the reduction of 4-NP with the activity factor of  $15.75 \text{ s}^{-1} \cdot \text{g}^{-1}$  [193]. AgNPs supported on xanthan gum (5.0–20.0 nm) could serve as a good catalyst for the reduction, and the large specific surface area of nanoparticles is favorable for the elevation of the efficiency [83]. *Portulaca arabinogalactan* stabilized AgNPs could facilitate electron transmission from  $\text{BH}_4^-$  to 4-NP thereby stimulating the reaction [97]. AuNPs stabilized by Locust bean gum, glucomannan and katira gum also revealed excellent catalytic ability in the reduction of 4-NP to 4-AP with their first-order rate constants were  $14.46 \times 10^{-2} \text{ min}^{-1}$ ,  $6.03 \times 10^{-3} \text{ s}^{-1}$  and  $2.67 \times 10^{-2} \text{ min}^{-1}$ , respectively [174,194,195]. Moreover, biometallic Ag-Au nanoparticles capped by hydroxyethyl starch-g-poly (11.1 nm) were synthesized and exhibited great recyclability (98–93%) after 4 cycles, providing an enhanced efficiency in the 4-NP reduction reaction [196].

Suzuki–Miyaura reaction, involving the C–C bond formation, is widely used for the synthesis of many carbon molecules, which is one of the most significant cross-coupling reaction [197]. The PdNPs catalysts are really unmatched choices for this reaction [198]. Recently, xylan-type hemicelluloses supported terpyridine-PdNPs showed high catalytic activity and stability for Suzuki–Miyaura reaction between arylboronic acid and aryl halide under aerobic condition, with a yield of 98%. It also could be recovered conveniently and rescued at least six times without significant changes in their catalytic activity [199]. PdNPs (3.0 nm) could form an alginate matrix with Cu alginate gels and resulted in an improvement in the activity and recyclability of Suzuki–Miyaura reaction [200]. Besides, starch derived PdNPs (1.5–4.5 nm) were tested in the microwave-assisted Heck, Suzuki and Sonogashira C–C coupling reactions and excellent catalytic performances were observed, confirming the catalytic potential of the Pd-supported catalysts [133].

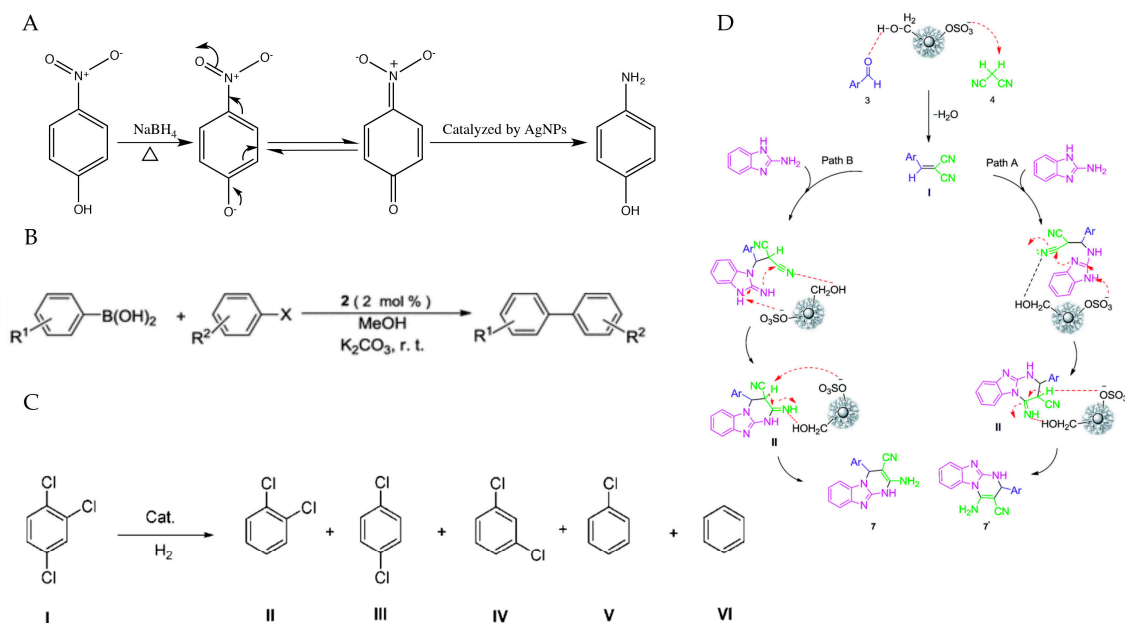


**Figure 7.** Overall scheme for the illustration of different catalytic reactions by PMNPs: **(A)** 4-NP reduction catalyzed by arabinogalactan stabilized AgNPs; **(B)** Suzuki coupling reaction of aryl halide with arylboronic acid catalyzed by xylan-type hemicelluloses supported terpyridine-PdNPs; **(C)** hydrogenation of 1,2,4-trichlorobenzene catalyzed by *Klebsiella oxytoca* BAS-10 exopolysaccharides supported PdFeNPs; and **(D)** Synthesis of imidazopyrimidine derivatives catalyzed by Irish moss/ $Fe_3O_4$  nanoparticles. Reproduced with permission [97,185,199,201].

*Klebsiella oxytoca* BAS-10 exopolysaccharides supported PdNPs and PdFeNPs were investigated for catalyzing the hydrogenation of *trans*-cinnamaldehyde and 1,2,4-trichlorobenzene, respectively. Results showed that these two PMNPs could stimulate the hydrogenation under mild reaction conditions and their catalytic activities were maintained after several recycle experiments [201,202]. PMNPs also revealed remarkable catalytic ability in the degradation of dyes [203,204]. In addition, esterification of palm fatty acid distillate, benzylation of *o*-xylene, toluene and ethylene glycol oxidation as well as synthesis of imidazopyrimidine derivatives could also be catalyzed by different PMNPs [185,205–208]. Nevertheless, there still exist some problems in the isolation and recovery of these tiny nano catalysts from the reaction mixture through conventional methods due to their nano size and solvation properties [185]. The improvement of the recovery efficiency is obviously a significant objective in further research.

**Table 5.** Summary of literature data regarding the catalytic property of PMNPs.

| Resource                         | Polysaccharides                            | Metals                         | Diameter (nm) | Shape                       | Reaction types                          | Reference |
|----------------------------------|--|--------------------------------|---------------|-----------------------------|---|-----------|
| -                                | Xanthan                                    | Ag                             | 5.0–40.0      | Spherical                   | 4-NP reduction                          | [83]      |
| <i>Portulaca</i>                 | Arabinogalactan                            | Ag                             | 20.0–30.0     | Spherical                   | 4-NP reduction                          | [97]      |
| -                                | Dextrin                                    | Ag/Au                          | 8.0–28.0      | Spherical                   | 4-NP reduction                          | [166]     |
| <i>Ceratonia siliqua</i>         | Locust bean gum                            | Au                             | -             | Spherical                   | 4-NP reduction                          | [174]     |
| <i>Chondrus crispus</i>          | Irish moss                                 | Fe <sub>3</sub> O <sub>4</sub> | -             | Homogeneous                 | Imidazopyrimidine derivatives synthesis | [185]     |
| -                                | Alginate                                   | Bi                             | 5.0–8.0       | Porous                      | 4-NP reduction                          | [192]     |
| <i>Cordyceps sinensis</i>        | Exopolysaccharides                         | Ag                             | 5.0           | Spherical                   | 4-NP reduction                          | [193]     |
| -                                | Glucomannan                                | Au                             | 12.0–31.0     | Spherical                   | 4-NP reduction                          | [194]     |
| <i>Cochlospermum religiosum</i>  | Katira gum                                 | Au                             | 6.9           | Spherical                   | 4-NP reduction                          | [195]     |
| -                                | Starch-g-poly                              | Ag-Au                          | 11.1          | -                           | 4-NP reduction                          | [196]     |
| -                                | Xylan-type hemicellulose                   | Terpyridine-Pd                 | 10.0–20.0     | Particle                    | Suzuki–Miyaura reaction                 | [199]     |
| -                                | Alginate                                   | Pd-Cu                          | >10           | Fibrils network             | Suzuki–Miyaura reaction                 | [200]     |
| <i>Klebsiella oxytoca</i> BAS-10 | Exopolysaccharides                         | Fe/Fe-Pd                       | 1.0–1.5       | Cluster                     | Hydrodechlorination reaction            | [201]     |
| <i>Klebsiella oxytoca</i> BAS-10 | Exopolysaccharides                         | Pd                             | 30.0–550.0    | Jagged undefined structures | Aqueous biphasic hydrogenation          | [202]     |
| -                                | Cellulose nanofibrils                      | Ag                             | 25.2–18.0     | Porous                      | Rhodamine B degradation                 | [203]     |
| Corn                             | Crosslinked carboxymethyl starch/cellulose | ZnO/Zn                         | 20.0–100.0    | Spherical                   | Photodegradation of dyes                | [204]     |
| Algae                            | Algin                                      | Al                             | 4.0–5.0       | Rough with wrinkled surface | Esterification reaction                 | [205]     |
| -                                | Chitosan                                   | ZrO                            | 9.0           | -                           | Benzylation of <i>o</i> -xylene         | [206]     |
| -                                | Sodium alginate                            | Cu-Mn                          | 10.0–20.0     | Spherical                   | Toluene oxidation                       | [207]     |

|  |  |         |           |  |   |       |
|--|--|---------|-----------|--|---|-------|
| -                                      | Dextrin                                      | Au      | 8.4–12.0  | -  | Liquid phase oxidation of ethylene glycol               | [208] |
| -                                      | Chitin                                       | Ag      | 5.5–15.2  | Mesoporous, fibrous                        | <i>p</i> -NP reduction                                  | [209] |
| -                                      | Salep  | Pd (II) | -         | Rough                                      | Suzuki coupling reaction                                | [210] |
| -                                      | Alginate                                     | Au      | 20.0–40.0 | Centered cubic crystal lattice             | Decoloration of Azo-Dyes                                | [211] |
| <i>Bupleurum falcatum</i>              | Water extract                                | Au      | 8.2–12.8  | Spherical                                  | 4-NP reduction  | [212] |
| <i>Acetobacter xylinum</i><br>NCIM2526 | Levan  | Ag/Au   | 5.0–12.0  | Spherical                                  | 4-NP reduction  | [213] |
| -                                      | Chitosan/<br>corn starch/<br>sodium alginate | ZnO     | 8.3–11.3  | Hexagonal phase with<br>Wurtzite structure | Photocatalytic reaction                                 | [214] |
| <i>Pleurotus florida</i>               | Glucan                                       | Au      | 19.0–27.2 | Spherical                                  | 4-NP reduction  | [215] |
| -                                      | Starch                                       | Pd      | 1.5–4.5   | Spherical                                  | Heck reaction, Suzuki<br>reaction, Sonogashira reaction | [216] |

## 5. Toxicity of PMNPs

There is no doubt that polysaccharide-based metallic nanoparticles have made significant progress in many areas. Similar to most new technologies, the majority investigations in PMNPs have been focused on their potential applications and limited information is available on their toxicity to the cell, animals and the environment. Currently, some excellent review articles have provided significant insights into the toxicological significance and proposed mechanisms [217,218]. In fact, the risks associated with exposure to nanoparticles, the possible entry ways and metabolic mechanism have not been clarified until now, and several reports have illustrated that the nanoparticles deposit were responsible for toxic damages in different organs [219–221]. Although polysaccharides are attractive due to their low-toxic property and apparent lack of side effects [222], it is still necessary to evaluate the potential risks and toxicity of PMNPs in details.

The major entry portals of PMNPs are respiratory system, oral ingestion, and skin absorption [204]. After being administered, the nanoparticles can be transported via blood circulation into different organs. It had been reported that the colloidal gold nanoparticles (30.0 nm) could be quickly observed in rat platelets after intratracheal instillation and Tc-labelled carbon particles (99.0 nm) could get into the blood circulation in 1 min [223,224]. Hemolysis, commonly known as the rupturing of red blood cells, can be induced by the oxidative-stress caused by nanoparticles, causing lysis and death of cells. Thus, the toxic effects of PMNPs were evaluated with reference to hemolysis percentage at first. Gum karaya-based AuPNs (15.0–20.0 nm) and xanthan-based AuPNs (20.0–25.0 nm) were found to display lower hemolysis rates, even at test concentrations over 200 µg/mL [155,225]. However, AgNPs (1.3–4.2 nm), use polysaccharides from edible mushroom *L. squarrosulus* (Mont.) Singer as the reducing and stabilizing agent, were found to be compatible with human red blood cells at a dose of less than 5 µg/mL [87]. Starch-based AgNPs (5.8 nm) could also induce significant hemolysis and exhibited a concentration-dependent in hemagglutination than AuNPs and PtNPs [226]. Therefore, the hemolysis risk assessment of PMNPs was needed before utilization. Other toxic effects of PMNPs were evaluated with the reference of cytotoxicity in normal cells. Accordingly, Gellan gum (10.0–15.0 nm) and Fucan (210.4 nm) coated AgNPs had a slight toxic effect towards to the mouse embryonic fibroblasts (NIH3T3) cells, human renal (HEK 293) cells and murine fibroblasts (3T3) cells [227,228]. Porphyrin (14.0 nm) and pectin (7.0–13.0 nm) based AuNPs had no significant changes in normal monkey kidney cells viability, even up to 100 µM concentration [229,230]. In addition, chitosan coated CuNPs (260.0 nm) could obviously increase the viability of human alveolar epithelial (A549) cells relative to the exposure of CuNPs. Inflammatory risks induced by chitosan coated CuNPs would be raised if administered via the lung [231]. Normally, macrophages will participate in the clearance of nanoparticles that have passed the mucociliary barrier, which will lead to the activation of pro-inflammatory mediators, causing both acute and chronic inflammation subsequently [232]. The investigations of inflammation in vitro, driven by PMNPs had showed that chitosan coated Ag/ZnO nanoparticles (100.0–150.0 nm) exerted no significant cytotoxic effects on murine macrophages RAW264.7 cells at the concentrations of 50 µg/mL and the cell morphology of cells was also not affected [74]. Additionally, PMNPs exhibited lower cytotoxicity than the metal itself, and different fluid exposure processes showed a significant effect on the viability of macrophage cells [233,234]. Several pieces of evidence also suggested that PMNPs had no neurotoxic effects and phyto-toxicity potential [235,236]. The sub-acute oral toxicity assessment also demonstrated the limited influences of PMNPs on the hematological and biochemical indexes of rats at the dose of 1500 ppm for 28 days [229,237]. Similar results were observed in the zebra fish toxicity study in vivo [238]. In addition, skin permeation study also showed that PMNPs could be detected in the receptor compartment in intact skin [227]. Although previous report had clarified that MNPs with the diameter smaller than 10.0 nm were able to penetrate the skin and reach the deepest layers of the stratum corneum, it did not permeate the skin [239].

Recent progresses in the toxicity investigation of PMNPs had put forward both the safety and risks at the same time. Nevertheless, it was still essential to consider the possible threaten that brought by MNPs in a long term exposure. Hence, more acute and sub-acute toxicity evaluation of PMNPs in vivo should be performed to avoid the potential hazards in the future.

## 6. Conclusions and Perspectives

As the research in MNPs increases, the awareness towards seeking renewable multifunctional hosts for the preparation of MNPs has increased in both academia and society. Using natural polysaccharides exhibited enormous potential in the green synthesis of MNPs owing to their non-toxic, biocompatible and biodegradable advantages. Through host–guest strategy, polysaccharides can act as the reducing and stabilizing agents of metallic ions and MNPs, providing an alternative way of solving the problems in conventional physical and chemical synthesis approaches. The present review has focused on the recent advances in the preparation, characterization and application of PMNPs. For the synthesis of MNPs employing natural polysaccharides through bottom-up synthesis approach can not only consume few chemicals and energy, but also showed a good control of the size and morphology property of MNPs. Despite the extensive applications of various techniques in the characterization of PMNPs, the combination of multiple techniques is considered to be more suitable for illustrating their properties because of their diverse and ambiguous properties. The illustration of the characteristics of the PMNPs will provide more insights into the synthesis mechanism, which will be beneficial to the targeted synthesis of the nanoparticles.

Although the development of green synthesis of PMNPs has achieved advanced progress, some problems still cannot be ignored. Due to significant variations in geography and time, the same species harvested in different seasons may lead to structural differences of the polysaccharides. Different synthesis methods of PMNPs also bring great challenges to their development and application. Thus, a commercially viable, eco-friendly and easy route for the synthesis of PMNPs is urgently needed. Another alternative attempt is to use synthetic polymers instead of the natural polysaccharides to synthesize PMNPs. The convenient management and adjustment of the synthetic process makes them to be a suitable host for the synthesis of homogeneous PMNPs.

Primarily PMNPs and their application in specific fields including wound healing, targeted delivery, biosensing, catalysis and agents with antimicrobial, antiviral and anticancer capabilities are well demonstrated in detail. The applications of the PMNPs are largely associated with the characteristics of the metallic ions. Therefore, the guest metallic ions that exhibited good property in the field of optics, images, diagnosis and nanomedicine shall be considered in the synthesis of PMNPs. On the other hand, the controversial toxicological evaluations of PMNPs in recent years are introduced both in vitro and in vivo. Long-term toxicity investigations, such as for acute and sub-acute toxicity evaluation of PMNPs, are still required to elucidate their potential risks. Despite the remarkable advances, the recovery efficiency of PMNPs remains low. Further investigations that introduce physical methods such as the recovery of magnetic PMNPs through an external magnetic field to improve the recovery efficiency are urgently needed. In addition, different methods that involve host–guest strategy in the synthesis of PMNPs are also encouraged.

**Acknowledgments:** This work was supported by the grant from the National Natural Science Foundation of China (NSFC 31371879) and National High Technology Research and Development Program (“863” Program) of China (Grant No. SS2013AA100207).

**Author Contributions:** Haixia Chen conceived and designed the manuscript; Cong Wang wrote the paper; Cong Wang, Xudong Gao and Zhongqin Chen contributed literature survey; and Xudong Gao, Zhongqin Chen and Yue Chen critically reviewed the manuscript.

**Conflicts of Interest:** The authors declare no conflict of interest.

## Abbreviations

The following abbreviations are used in this manuscript: Metallic nanoparticles, MNPs; Polysaccharides based metallic nanoparticles, PMNPs; Confocal laser scanning microscopy, CLSM; Scan electron microscopy, SEM; Transmission electron microscopy, TEM; X-ray diffraction, XRD; small-angle X-ray scattering, SAXS; Scanning tunneling microscopy, STM; Dynamic light scattering, DLS; Atomic-force microscopy, AFM; Electron spin resonance, ESR; Minimum inhibitory concentration, MIC; Fourier transform infrared spectroscopy, FTIR; Reactive oxygen species, ROS; Human immunodeficiency virus, HIV; Severe acute respiratory syndrome, SARS; 3-(4,5-dimethylthiazol-2-yl)-2,5-diphenyltetrazolium bromide, MTT; Hematoxylin & eosin, H&E; *Escherichia coli*,

*E. coli*; *Staphylococcus epidermidis*, *S. epidermidis*; *Staphylococcus aureus*, *S. aureus*; *Pseudomonas aeruginosa*, *P. aeruginosa*; *Sarcina lutea*, *S. lutea*; *Bacillus subtilis*, *B. subtilis*; *Klebsiella planticola*, *K. planticola*; *Klebsiella pneumoniae*, *K. pneumoniae*; *Candida albicans*, *C. albicans*; *Fusarium oxysporum*, *F. oxysporum*; *Lactobacillus fermentum*, *L. fermentum*; *Enterococcus faecium*, *E. faecium*; *Bacillus licheniformis*, *B. licheniformis*; *Bacillus cereus*, *B. cereus*; *Vibrio parahaemolyticus*, *V. parahaemolyticus*; *Proteus vulgaris*, *P. vulgaris*; *Salmonella typhimurium*, *S. typhimurium*; *Kocuria rhizophila*, *K. rhizophila*; *Aeromonas hydrophila*, *A. hydrophila*; *Streptococcus pyogenes*, *S. pyogenes*; *Aspergillus niger*, *A. niger*; *Trichophyton rubrum*, *T. rubrum*; *Vibrio cholerae*, *V. cholerae*; *Streptococcus pneumoniae*, *S. pneumoniae*; *Listeria monocytogenes*, *L. monocytogenes*; *Enterococcus faecalis*, *E. faecalis*; *Candida krusei*, *C. krusei*; *Saccharomyces cerevisiae*, *S. cerevisiae*; *Aspergillus flavus*, *A. flavus*.

## References

- Datta, K.K.R.; Reddy, B.V.S.; Zboril, R. Polysaccharides as functional scaffolds for noble metal nanoparticles and their catalytic applications. In *Encyclopedia of Nanoscience and Nanotechnology*; American Scientific Publishers: Valencia, CA, USA, 2016; pp. 1–20, ISBN 1588831590.
- Huang, H.; Yuan, Q.; Yang, X. Preparation and characterization of metal-chitosan nanocomposites. *Colloids Surf. B Biointerfaces* **2004**, *39*, 31–37.
- Huang, X.; Jain, P.K.; El-Sayed, I.H.; El-Sayed, M.A. Plasmonic photothermal therapy (PPTT) using gold nanoparticles. *Lasers Med. Sci.* **2008**, *23*, 217–228.
- Sengupta, S.; Eavarone, D.; Capila, I.; Zhao, G.; Watson, N.; Kiziltepe, T.; Sasisekharan, R. Temporal targeting of tumour cells and neovasculature with a nanoscale delivery system. *Nature* **2005**, *436*, 568–572.
- Neville, F.; Pchelintsev, N.A.; Broderick, M.J.F.; Gibson, T.; Millner, P.A. Novel one-pot synthesis and characterization of bioactive thiol-silicate nanoparticles for biocatalytic and biosensor applications. *Nanotechnology* **2009**, *20*, 55612.
- Ahmed, S.; Ahmad, M.; Swami, B.L.; Ikram, S. Green synthesis of silver nanoparticles using *Azadirachta indica* aqueous leaf extract. *J. Radiat. Res. Appl. Sci.* **2016**, *9*, 1–7.
- Medina-Ramirez, I.; Bashir, S.; Luo, Z.; Liu, J.L. Green synthesis and characterization of polymer-stabilized silver nanoparticles. *Colloids Surf. B Biointerfaces* **2009**, *73*, 185–191.
- Zhao, C.; Li, J.; He, B.; Zhao, L. Fabrication of hydrophobic biocomposite by combining cellulosic fibers with polyhydroxyalkanoate. *Cellulose* **2017**, *24*, 2265–2274.
- Siqueira, G.; Bras, J.; Dufresne, A. Cellulosic bionanocomposites: A review of preparation, properties and applications. *Polymers* **2010**, *2*, 728–765.
- Pauly, M.; Keegstra, K. Cell-wall carbohydrates and their modification as a resource for biofuels. *Plant J.* **2008**, *54*, 559–568.
- Emna, C.; Fatma, G.; Satinder, K.B. Biopolymers Synthesis and Application. In *Biotransformation of Waste Biomass into High Value Biochemicals*; Springer: New York, NY, USA, 2014; Chapter 17, pp. 415–443, ISBN 9781461480051.
- Pasqui, D.; De Cagna, M.; Barbucci, R. Polysaccharide-based hydrogels: The key role of water in affecting mechanical properties. *Polymers* **2012**, *4*, 1517–1534.
- Liu, Z.; Jiao, Y.; Wang, Y.; Zhou, C.; Zhang, Z. Polysaccharides-based nanoparticles as drug delivery systems. *Adv. Drug Deliv. Rev.* **2008**, *60*, 1650–1662.
- Yang, J.; Han, S.; Zheng, H.; Dong, H.; Liu, J. Preparation and application of micro/nanoparticles based on natural polysaccharides. *Carbohydr. Polym.* **2015**, *123*, 53–66.
- Lee, J.W.; Park, J.H.; Robinson, J.R. Bioadhesive-based dosage forms: The next generation. *J. Pharm. Sci.* **2000**, *89*, 850–866.
- Debele, T.A.; Mekuria, S.L.; Tsai, H.C. Polysaccharide based nanogels in the drug delivery system: Application as the carrier of pharmaceutical agents. *Mater. Sci. Eng. C* **2016**, *68*, 964–981.
- Wang, J.; Chen, H.; Wang, Y.; Xing, L. Synthesis and characterization of a new *Inonotus obliquus* polysaccharide-iron(III) complex. *Int. J. Biol. Macromol.* **2015**, *75*, 210–217.
- Li, W.; Yuan, G.; Pan, Y.; Wang, C.; Chen, H. Network Pharmacology Studies on the Bioactive Compounds and Action Mechanisms of Natural Products for the Treatment of Diabetes Mellitus: A Review. *Front. Pharmacol.* **2017**, *8*, 1–10.
- Wang, C.; Chen, Z.; Pan, Y.; Gao, X.; Chen, H. Anti-diabetic effects of *Inonotus obliquus* polysaccharides-chromium(III) complex in type 2 diabetic mice and its sub-acute toxicity evaluation in normal mice. *Food Chem. Toxicol.* **2017**, *108*, 498–509.

20. Rao, K.M.; Kumar, A.; Haider, A.; Han, S.S. Polysaccharides based antibacterial polyelectrolyte hydrogels with silver nanoparticles. *Mater. Lett.* **2016**, *184*, 189–192.
21. Kim, C.; Tonga, G.Y.; Yan, B.; Kim, C.S.; Kim, S.T.; Park, M.-H.; Zhu, Z.; Duncan, B.; Creran, B.; Rotello, V.M. Regulating exocytosis of nanoparticles via host–guest chemistry. *Org. Biomol. Chem.* **2015**, *13*, 2474–2479.
22. Dhar, S.; Maheswara Reddy, E.; Shiras, A.; Pokharkar, V.; Prasad, B.L. Natural gum reduced/stabilized gold nanoparticles for drug delivery formulations. *Chemistry* **2008**, *14*, 10244–10250.
23. Tran, H.V.; Tran, L.D.; Ba, C.T.; Vu, H.D.; Nguyen, T.N.; Pham, D.G.; Nguyen, P.X. Synthesis, characterization, antibacterial and antiproliferative activities of monodisperse chitosan- based silver nanoparticles. *Colloids Surf. A Physicochem. Eng. Asp.* **2010**, *360*, 32–40.
24. Narayanan, G.; Aguda, R.; Hartman, M.; Chung, C.C.; Boy, R.; Gupta, B.S.; Tonelli, A.E. Fabrication and Characterization of Poly( $\epsilon$ -caprolactone)/ $\alpha$ -Cyclodextrin Pseudorotaxane Nanofibers. *Biomacromolecules* **2016**, *17*, 271–279.
25. Moreno-Trejo, M.B.; Sánchez-Domínguez, M. Mesquite gum as a novel reducing and stabilizing agent for modified tollens synthesis of highly concentrated Ag nanoparticles. *Materials* **2016**, *9*, 817.
26. Chen, W.H.; Lei, Q.; Luo, G.F.; Jia, H.Z.; Hong, S.; Liu, Y.X.; Cheng, Y.J.; Zhang, X.Z. Rational Design of Multifunctional Gold Nanoparticles via Host-Guest Interaction for Cancer-Targeted Therapy. *ACS Appl. Mater. Interfaces* **2015**, *7*, 17171–17180.
27. Noël, S.; Léger, B.; Ponchel, A.; Philippot, K.; Denicourt-Nowicki, A.; Roucoux, A.; Monflier, E. Cyclodextrin-based systems for the stabilization of metallic(0) nanoparticles and their versatile applications in catalysis. *Catal. Today* **2014**, *235*, 20–32.
28. Yao, X.; Zhu, Q.; Li, C.; Yuan, K.; Che, R.; Zhang, P.; Yang, C.; Lu, W.; Wu, W.; Jiang, X. Carbamoylmannose enhances the tumor targeting ability of supramolecular nanoparticles formed through host–guest complexation of a pair of homopolymers. *J. Mater. Chem. B* **2017**, *5*, 834–848.
29. Nair, L.S.; Laurencin, C.T. Silver nanoparticles: Synthesis and therapeutic applications. *J. Biomed. Nanotechnol.* **2007**, *3*, 301–316.
30. Sharma, D.; Kanchi, S.; Bisetty, K. Biogenic synthesis of nanoparticles: A review. *Arab. J. Chem.* **2015**, doi:10.1016/j.arabjc.2015.11.002.
31. Ahmed, S.; Ahmad, M.; Swami, B.L.; Ikram, S. A review on plants extract mediated synthesis of silver nanoparticles for antimicrobial applications: A green expertise. *J. Adv. Res.* **2016**, *7*, 17–28.
32. Kaliaraj, G.S.; Subramaniyan, B.; Manivasagan, P. Green Synthesis of Metal Nanoparticles Using Seaweed Polysaccharides. In *Seaweed Polysaccharides*; Elsevier: Amsterdam, The Netherlands, 2017; Chapter 7, pp. 101–109, ISBN 9780128098165.
33. Shukla, A.K.; Irvani, S. Metallic nanoparticles: Green synthesis and spectroscopic characterization. *Environ. Chem. Lett.* **2017**, *15*, 223–231.
34. Singh, P.; Kim, Y.J.; Zhang, D.; Yang, D.C. Biological Synthesis of Nanoparticles from Plants and Microorganisms. *Trends Biotechnol.* **2016**, *34*, 588–599.
35. Thakkar, K.N.; Mhatre, S.S.; Parikh, R.Y. Biological synthesis of metallic nanoparticles. *Nanomed. Nanotechnol. Biol. Med.* **2010**, *6*, 257–262.
36. Mittal, A.K.; Chisti, Y.; Banerjee, U.C. Synthesis of metallic nanoparticles using plant extracts. *Biotechnol. Adv.* **2013**, *31*, 346–356.
37. Yip, J.; Liu, L.; Wong, K.H.; Leung, P.H.M.; Yuen, C.W.M.; Cheung, M.C. Investigation of antifungal and antibacterial effects of fabric padded with highly stable selenium nanoparticles. *J. Appl. Polym. Sci.* **2014**, *131*, 8886–8893.
38. Li, H.; Yang, Y.W. Gold nanoparticles functionalized with supramolecular macrocycles. *Chin. Chem. Lett.* **2013**, *24*, 545–552.
39. Cram, D.J.; Cram, J.M. Host-Guest Chemistry. *Science* **1974**, *183*, 803–809.
40. Niu, Z.; Li, Y. Removal and utilization of capping agents in nanocatalysis. *Chem. Mater.* **2014**, *26*, 72–83.
41. Chan, H.K.; Kwok, P.C.L. Production methods for nanodrug particles using the bottom-up approach. *Adv. Drug Deliv. Rev.* **2011**, *63*, 406–416.
42. Raghunandan, D.; Basavaraja, S.; Mahesh, B.; Balaji, S.; Manjunath, S.Y.; Venkataraman, A. Biosynthesis of stable polyshaped gold nanoparticles from microwave-exposed aqueous extracellular anti-malignant guava (*Psidium guajava*) leaf extract. *Nanobiotechnology* **2009**, *5*, 34–41.



43. Hussain, M.A.; Shah, A.; Jantan, I.; Shah, M.R.; Tahir, M.N.; Ahmad, R.; Bukhari, S.N.A. Hydroxypropylcellulose as a novel green reservoir for the synthesis, stabilization, and storage of silver nanoparticles. *Int. J. Nanomed.* **2015**, *10*, 2079–2088.
44. Ehmann, H.M.A.; Breitwieser, D.; Winter, S.; Gspan, C.; Koraimann, G.; Maver, U.; Segal, M.; Köstler, S.; Stana-Kleinschek, K.; Spirk, S.; et al. Gold nanoparticles in the engineering of antibacterial and anticoagulant surfaces. *Carbohydr. Polym.* **2015**, *117*, 34–42.
45. Abedini, A.; Daud, A.; Abdul Hamid, M.; Kamil Othman, N.; Saion, E. A review on radiation-induced nucleation and growth of colloidal metallic nanoparticles. *Nanoscale Res. Lett.* **2013**, *8*, 474.
46. Irvani, S.; Korbekandi, H.; Mirmohammadi, S.V.; Zolfaghari, B. Synthesis of silver nanoparticles: Chemical, physical and biological methods. *Res. Pharm. Sci.* **2014**, *9*, 385–406.
47. Sokolov, S.V.; Batchelor-McAuley, C.; Tschulik, K.; Fletcher, S.; Compton, R.G. Are Nanoparticles Spherical or Quasi-Spherical? *Chemistry* **2015**, *21*, 10741–10746.
48. Lechner, M.; Mächtle, W. Characterization of nanoparticles. *Macromol. Symp.* **1999**, *7*, 1–7.
49. Hall, J.B.; Dobrovolskaia, M.A.; Patri, A.K.; McNeil, S.E. Characterization of nanoparticles for therapeutics. *Nanomedicine* **2007**, *2*, 789–803.
50. Bootz, A.; Vogel, V.; Schubert, D.; Kreuter, J. Comparison of scanning electron microscopy, dynamic light scattering and analytical ultracentrifugation for the sizing of poly(butyl cyanoacrylate) nanoparticles. *Eur. J. Pharm. Biopharm.* **2004**, *57*, 369–375.
51. Lin, P.C.; Lin, S.; Wang, P.C.; Sridhar, R. Techniques for physicochemical characterization of nanomaterials. *Biotechnol. Adv.* **2014**, *32*, 711–726.
52. Dobrovolskaia, M.A.; Patri, A.K.; Zheng, J.; Clogston, J.D.; Ayub, N.; Aggarwal, P.; Neun, B.W.; Hall, J.B.; McNeil, S.E. Interaction of colloidal gold nanoparticles with human blood: Effects on particle size and analysis of plasma protein binding profiles. *Nanomed. Nanotechnol. Biol. Med.* **2009**, *5*, 106–117.
53. Powers, K.W.; Palazuelos, M.; Moudgil, B.M.; Roberts, S.M. Characterization of the size, shape, and state of dispersion of nanoparticles for toxicological studies. *Nanotoxicology* **2007**, *1*, 42–51.
54. Sanyasi, S.; Majhi, R.K.; Kumar, S.; Mishra, M.; Ghosh, A.; Suar, M.; Satyam, P.V.; Mohapatra, H.; Goswami, C.; Goswami, L. Polysaccharide-capped silver Nanoparticles inhibit biofilm formation and eliminate multi-drug-resistant bacteria by disrupting bacterial cytoskeleton with reduced cytotoxicity towards mammalian cells. *Sci. Rep.* **2016**, *6*, 24929.
55. Berne, B.J.; Pecora, R. *Dynamic Light Scattering: With Applications to Chemistry, Biology, and Physics*, 1st ed.; Dover Publ.: New York, NY, USA, 2000; pp. 3–24, ISBN 0486411559.
56. Ito, T.; Sun, L.; Bevan, M.A.; Crooks, R.M. Comparison of nanoparticle size and electrophoretic mobility measurements using a carbon-nanotube-based coulter counter, dynamic light scattering, transmission electron microscopy, and phase analysis light scattering. *Langmuir* **2004**, *20*, 6940–6945.
57. Upstone, S. Ultraviolet/visible light absorption spectrophotometry in clinical chemistry. *Encycl. Anal. Chem.* **2000**, 1699–1714, doi:10.1002/9780470027318.a0547.
58. Liu, X.M.; Sheng, G.P.; Luo, H.W.; Zhang, F.; Yuan, S.J.; Xu, J.; Zeng, R.J.; Wu, J.G.; Yu, H.Q. Contribution of extracellular polymeric substances (EPS) to the sludge aggregation. *Environ. Sci. Technol.* **2010**, *44*, 4355–4360.
59. Khorsand Zak, A.; Abd. Majid, W.H.; Abrishami, M.E.; Yousefi, R. X-ray analysis of ZnO nanoparticles by Williamson-Hall and size-strain plot methods. *Solid State Sci.* **2011**, *13*, 251–256.
60. Sapsford, K.E.; Tyner, K.M.; Dair, B.J.; Deschamps, J.R.; Medintz, I.L. Analyzing nanomaterial bioconjugates: A review of current and emerging purification and characterization techniques. *Anal. Chem.* **2011**, *83*, 4453–4488.
61. Caminade, A.M.; Laurent, R.; Majoral, J.P. Characterization of dendrimers. *Adv. Drug Deliv. Rev.* **2005**, *57*, 2130–2146.
62. Stanjek, H.; Häusler, W. Basics of X-ray diffraction. *Hyperfine Interact.* **2004**, *154*, 107–119.
63. Bindu, P.; Thomas, S. Estimation of lattice strain in ZnO nanoparticles: X-ray peak profile analysis. *J. Theor. Appl. Phys.* **2014**, *8*, 123–134.
64. Tadic, M.; Panjan, M.; Damnjanovic, V.; Milosevic, I. Magnetic properties of hematite ( $\alpha$ -Fe<sub>2</sub>O<sub>3</sub>) nanoparticles prepared by hydrothermal synthesis method. *Appl. Surf. Sci.* **2014**, *320*, 183–187.
65. Das, T.; Yeasmin, S.; Khatua, S.; Acharya, K.; Bandyopadhyay, A. Influence of a blend of guar gum and poly(vinyl alcohol) on long term stability, and antibacterial and antioxidant efficacies of silver nanoparticles. *RSC Adv.* **2015**, *5*, 54059–54069.

66. Gupta, D.; Singh, D.; Kothiyal, N.C.; Saini, A.K.; Singh, V.P.; Pathania, D. Synthesis of chitosan-g-poly(acrylamide)/ZnS nanocomposite for controlled drug delivery and antimicrobial activity. *Int. J. Biol. Macromol.* **2015**, *74*, 547–557.
67. Vidya, S.M.; Mutalik, S.; Bhat, K.U.; Huilgol, P.; Avadhani, K. Preparation of gold nanoparticles by novel bacterial exopolysaccharide for antibiotic delivery. *Life Sci.* **2016**, *153*, 171–179.
68. El-Rafie, M.H.; Mohamed, A.A.; Shaheen, T.I.; Hebeish, A. Antimicrobial effect of silver nanoparticles produced by fungal process on cotton fabrics. *Carbohydr. Polym.* **2010**, *80*, 779–782.
69. Ma, Y.; Liu, C.; Qu, D.; Chen, Y.; Huang, M.; Liu, Y. Antibacterial evaluation of silver nanoparticles synthesized by polysaccharides from *Astragalus membranaceus* roots. *Biomed. Pharmacother.* **2017**, *89*, 351–357.
70. Kanmani, P.; Lim, S.T. Synthesis and characterization of pullulan-mediated silver nanoparticles and its antimicrobial activities. *Carbohydr. Polym.* **2013**, *97*, 421–428.
71. Chopra, I. The increasing use of silver-based products as antimicrobial agents: A useful development or a cause for concern? *J. Antimicrob. Chemother.* **2007**, *59*, 587–590.
72. Gwinn, E.G.; O'Neill, P.; Guerrero, A.J.; Bouwmeester, D.; Fygenson, D.K. Sequence-dependent fluorescence of DNA-hosted silver nanoclusters. *Adv. Mater.* **2008**, *20*, 279–283.
73. Pallavicini, P.; Arciola, C.R.; Bertoglio, F.; Curtosi, S.; Dacarro, G.; D'Agostino, A.; Ferrari, F.; Merli, D.; Milanese, C.; Rossi, S.; et al. Silver nanoparticles synthesized and coated with pectin: An ideal compromise for anti-bacterial and anti-biofilm action combined with wound-healing properties. *J. Colloid Interface Sci.* **2017**, *498*, 271–281.
74. Thaya, R.; Malaikozhundan, B.; Vijayakumar, S.; Sivakamavalli, J.; Jeyasekar, R.; Shanthi, S.; Vaseeharan, B.; Ramasamy, P.; Sonawane, A. Chitosan coated Ag/ZnO nanocomposite and their antibiofilm, antifungal and cytotoxic effects on murine macrophages. *Microb. Pathog.* **2016**, *100*, 124–132.
75. Sathiyarayanan, G.; Vignesh, V.; Saibaba, G.; Vinothkanna, A.; Dineshkumar, K.; Viswanathan, M.B.; Selvin, J. Synthesis of carbohydrate polymer encrusted gold nanoparticles using bacterial exopolysaccharide: A novel and greener approach. *RSC Adv.* **2014**, *4*, 22817–22827.
76. Geraldo, D.A.; Needhan, P.; Chandia, N.; Arratia-Pérez, R.; Mora, G.C.; Villagra, N. Green synthesis of polysaccharides-based gold and silver nanoparticles and their promissory biological activity. *Biointerface Res. Appl. Chem.* **2016**, *6*, 1263–1271.
77. Valodkar, M.; Rathore, P.S.; Jadeja, R.N.; Thounaojam, M.; Devkar, R.V.; Thakore, S. Cytotoxicity evaluation and antimicrobial studies of starch capped water soluble copper nanoparticles. *J. Hazard. Mater.* **2012**, *201–202*, 244–249.
78. Rajeshkumar, S. Phytochemical constituents of fucoidan (*Padina tetrastromatica*) and its assisted AgNPs for enhanced antibacterial activity. *IET Nanobiotechnol.* **2016**, *11*, 292–299.
79. Goyal, G.; Hwang, J.; Aviral, J.; Seo, Y.; Jo, Y.; Son, J.; Choi, J. Green synthesis of silver nanoparticles using  $\beta$ -glucan, and their incorporation into doxorubicin-loaded water-in-oil nanoemulsions for antitumor and antibacterial applications. *J. Ind. Eng. Chem.* **2017**, *47*, 179–186.
80. Yumei, L.; Yamei, L.; Qiang, L.; Jie, B. Rapid Biosynthesis of Silver Nanoparticles Based on Flocculation and Reduction of an Exopolysaccharide from *Arthrobacter* sp. B4: Its Antimicrobial Activity and Phytotoxicity. *J. Nanomater.* **2017**, *2017*, 9703614.
81. Chen, X.; Yan, J.-K.; Wu, J.-Y. Characterization and antibacterial activity of silver nanoparticles prepared with a fungal exopolysaccharide in water. *Food Hydrocoll.* **2015**, *53*, 69–74.
82. Emam, H.E.; Zahran, M.K. Ag<sup>0</sup> nanoparticles containing cotton fabric: Synthesis, characterization, color data and antibacterial action. *Int. J. Biol. Macromol.* **2015**, *75*, 106–114.
83. Xu, W.; Jin, W.; Lin, L.; Zhang, C.; Li, Z.; Li, Y.; Song, R.; Li, B. Green synthesis of xanthan conformation-based silver nanoparticles: Antibacterial and catalytic application. *Carbohydr. Polym.* **2014**, *101*, 961–967.
84. Ghasemzadeh, H.; Mahboubi, A.; Karimi, K.; Hassani, S. Full polysaccharide chitosan-CMC membrane and silver nanocomposite: Synthesis, characterization, and antibacterial behaviors. *Polym. Adv. Technol.* **2016**, *27*, 1204–1210.
85. Rasulov, B.; Rustamova, N.; Yili, A.; Zhao, H.Q.; Aisa, H.A. Synthesis of silver nanoparticles on the basis of low and high molar mass exopolysaccharides of *Bradyrhizobium japonicum* 36 and its antimicrobial activity against some pathogens. *Folia Microbiol.* **2016**, *61*, 283–293.

86. Baldi, F.; Daniele, S.; Gallo, M.; Paganelli, S.; Battistel, D.; Piccolo, O.; Faleri, C.; Puglia, A.M.; Gallo, G. Polysaccharide-based silver nanoparticles synthesized by *Klebsiella oxytoca* DSM 29614 cause DNA fragmentation in *E. coli* cells. *BioMetals* **2016**, *29*, 321–331.
87. Manna, D.K.; Mandal, A.K.; Sen, I.K.; Maji, P.K.; Chakraborti, S.; Chakraborty, R.; Islam, S.S. Antibacterial and DNA degradation potential of silver nanoparticles synthesized via green route. *Int. J. Biol. Macromol.* **2015**, *80*, 455–459.
88. Sen, I.K.; Mandal, A.K.; Chakraborti, S.; Dey, B.; Chakraborty, R.; Islam, S.S. Green synthesis of silver nanoparticles using glucan from mushroom and study of antibacterial activity. *Int. J. Biol. Macromol.* **2013**, *62*, 439–449.
89. Kanmani, P.; Lim, S.T. Synthesis and structural characterization of silver nanoparticles using bacterial exopolysaccharide and its antimicrobial activity against food and multidrug resistant pathogens. *Process Biochem.* **2013**, *48*, 1099–1106.
90. Iconaru, S.L.; Prodan, A.M.; Motelica-Heino, M.; Sizaret, S.; Predoi, D. Synthesis and characterization of polysaccharide-maghemite composite nanoparticles and their antibacterial properties. *Nanoscale Res. Lett.* **2012**, *7*, 576.
91. White, R.J.; Budarin, V.L.; Moir, J.W.B.; Clark, J.H. A sweet killer: Mesoporous polysaccharide confined silver nanoparticles for antibacterial applications. *Int. J. Mol. Sci.* **2011**, *12*, 5782–5796.
92. Kora, A.; Beedu, S.; Jayaraman, A. Size-controlled green synthesis of silver nanoparticles mediated by gum ghatti (*Anogeissus latifolia*) and its biological activity. *Org. Med. Chem. Lett.* **2012**, *2*, 17.
93. El-Rafie, H.M.; El-Rafie, M.H.; Zahran, M.K. Green synthesis of silver nanoparticles using polysaccharides extracted from marine macro algae. *Carbohydr. Polym.* **2013**, *96*, 403–410.
94. Selvakumar, R.; Aravindh, S.; Ashok, A.M.; Balachandran, Y.L. A facile synthesis of silver nanoparticle with SERS and antimicrobial activity using *Bacillus subtilis* exopolysaccharides. *J. Exp. Nanosci.* **2013**, *8080*, 1–13.
95. Kora, A.J.; Sashidhar, R.B.; Arunachalam, J. Gum kondagogu (*Cochlospermum gossypium*): A template for the green synthesis and stabilization of silver nanoparticles with antibacterial application. *Carbohydr. Polym.* **2010**, *82*, 670–679.
96. Venkatpurwar, V.; Pokharkar, V. Green synthesis of silver nanoparticles using marine polysaccharide: Study of in-vitro antibacterial activity. *Mater. Lett.* **2011**, *65*, 999–1002.
97. Anuradha, K.; Bangal, P.; Madhavendra, S.S. Macromolecular arabinogalactan polysaccharide mediated synthesis of silver nanoparticles, characterization and evaluation. *Macromol. Res.* **2016**, *24*, 152–162.
98. Gostin, L.O.; Hodge, J.G. Zika virus and global health security. *Lancet Infect. Dis.* **2016**, *16*, 1099–1100.
99. Koonin, E.V.; Senkevich, T.G.; Dolja, V.V. The ancient Virus World and evolution of cells. *Biol. Direct* **2006**, *1*, 29.
100. Zheng, L.; Wei, J.; Lv, X.; Bi, Y.; Wu, P.; Zhang, Z.; Wang, P.; Liu, R.; Jiang, J.; Cong, H.; et al. Detection and differentiation of influenza viruses with glycan-functionalized gold nanoparticles. *Biosens. Bioelectron.* **2017**, *91*, 46–52.
101. Wei, J.; Zheng, L.; Lv, X.; Bi, Y.; Chen, W.; Zhang, W.; Shi, Y.; Zhao, L.; Sun, X.; Wang, F.; et al. Analysis of Influenza Virus Receptor Specificity Using Glycan-Functionalized Gold Nanoparticles. *ACS Nano* **2014**, *8*, 4600–4607.
102. Yan, J.-K.; Ma, H.-L.; Cai, P.-F.; Wu, J.-Y. Highly selective and sensitive nucleic acid detection based on polysaccharide-functionalized silver nanoparticles. *Spectrochim. Acta Part A Mol. Biomol. Spectrosc.* **2015**, *134*, 17–21.
103. Speshock, J.L.; Murdock, R.C.; Braydich-Stolle, L.K.; Schrand, A.M.; Hussain, S.M. Interaction of silver nanoparticles with Tacaribe virus. *J. Nanobiotechnol.* **2010**, *8*, 19.
104. Rogers, J.V.; Parkinson, C.V.; Choi, Y.W.; Speshock, J.L.; Hussain, S.M. A preliminary assessment of silver nanoparticle inhibition of monkeypox virus plaque formation. *Nanoscale Res. Lett.* **2008**, *3*, 129–133.
105. Chen, Y.-S.; Hung, Y.-C.; Lin, W.-H.; Huang, G.S. Assessment of gold nanoparticles as a size-dependent vaccine carrier for enhancing the antibody response against synthetic foot-and-mouth disease virus peptide. *Nanotechnology* **2010**, *21*, 195101.
106. Zheng, Y.; Wang, W.; Li, Y. Antitumor and immunomodulatory activity of polysaccharide isolated from *Trametes orientalis*. *Carbohydr. Polym.* **2015**, *131*, 248–254.

107. Tietze, R.; Zaloga, J.; Unterweger, H.; Lyer, S.; Friedrich, R.P.; Janko, C.; Pöttler, M.; Dürr, S.; Alexiou, C. Magnetic nanoparticle-based drug delivery for cancer therapy. *Biochem. Biophys. Res. Commun.* **2015**, *468*, 463–470.
108. Wicki, A.; Witzigmann, D.; Balasubramanian, V.; Huwyler, J. Nanomedicine in Cancer Therapy: Challenges, Opportunities, and Clinical Applications. *J. Control. Release* **2014**, *200*, 138–157.
109. Joseph, M.M.; Aravind, S.R.; George, S.K.; Pillai, K.R.; Mini, S.; Sreelekha, T.T. Antitumor activity of galactoxyloglucan-gold nanoparticles against murine ascites and solid carcinoma. *Colloids Surf. B Biointerfaces* **2014**, *116*, 219–227.
110. Suganya, K.S.U.; Govindaraju, K.; Kumar, V.G.; Karthick, V.; Parthasarathy, K. Pectin mediated gold nanoparticles induces apoptosis in mammary adenocarcinoma cell lines. *Int. J. Biol. Macromol.* **2016**, *93*, 1030–1040.
111. Joseph, M.M.; Aravind, S.R.; Varghese, S.; Mini, S.; Sreelekha, T.T. PST-Gold nanoparticle as an effective anticancer agent with immunomodulatory properties. *Colloids Surf. B Biointerfaces* **2013**, *104*, 32–39.
112. Tengdelius, M.; Gurav, D.; Konradsson, P.; Pålsson, P.; Griffith, M.; Oommen, O.P. Synthesis and anticancer properties of fucoidan-mimetic glycopolymers coated gold nanoparticles. *Chem. Commun.* **2015**, *2*, 8532–8535.
113. Chen, T.; Wong, Y.S. Selenocystine induces apoptosis of A375 human melanoma cells by activating ROS-mediated mitochondrial pathway and p53 phosphorylation. *Cell. Mol. Life Sci.* **2008**, *65*, 2763–2775.
114. Nie, T.; Wu, H.; Wong, K.-H.; Chen, T. Facile synthesis of highly uniform selenium nanoparticles using glucose as the reductant and surface decorator to induce cancer cell apoptosis. *J. Mater. Chem. B* **2016**, *4*, 2351–2358.
115. Budihardjo, I.; Oliver, H.; Lutter, M.; Luo, X.; Wang, X. Biochemical pathways of caspase activation during apoptosis. *Annu. Rev. Cell Dev. Biol.* **1999**, *15*, 269–290.
116. Namvar, F.; Rahman, H.S.; Mohamad, R.; Baharara, J.; Mahdavi, M.; Amini, E.; Chartrand, M.S.; Yeap, S.K. Cytotoxic effect of magnetic iron oxide nanoparticles synthesized via seaweed aqueous extract. *Int. J. Nanomed.* **2014**, *9*, 2479–2488.
117. Wu, H.; Zhu, H.; Li, X.; Liu, Z.; Zheng, W.; Chen, T.; Yu, B.; Wong, K.H. Induction of apoptosis and cell cycle arrest in A549 human lung adenocarcinoma cells by surface-capping selenium nanoparticles: An effect enhanced by polysaccharide-protein complexes from *Polyporus rhinoceros*. *J. Agric. Food Chem.* **2013**, *61*, 9859–9866.
118. Raveendran, S.; Chauhan, N.; Palaninathan, V.; Nagaoka, Y.; Yoshida, Y.; Maekawa, T.; Kumar, D.S. Extremophilic polysaccharide for biosynthesis and passivation of gold nanoparticles and photothermal ablation of cancer cells. *Part. Part. Syst. Charact.* **2015**, *32*, 54–64.
119. Liu, C.P.; Lin, F.S.; Chien, C.T.; Tseng, S.Y.; Luo, C.W.; Chen, C.H.; Chen, J.K.; Tseng, F.G.; Hwu, Y.; Lo, L.W.; et al. In-situ formation and assembly of gold nanoparticles by gum Arabic as efficient photothermal agent for killing cancer cells. *Macromol. Biosci.* **2013**, *13*, 1314–1320.
120. Medhat, D.; Hussein, J.; El-Naggar, M.E.; Attia, M.F.; Anwar, M.; Latif, Y.A.; Booles, H.F.; Morsy, S.; Farrag, A.R.; Khalil, W.K.B.; et al. Effect of Au-dextran NPs as anti-tumor agent against EAC and solid tumor in mice by biochemical evaluations and histopathological investigations. *Biomed. Pharmacother.* **2017**, *91*, 1006–1016.
121. Arjunan, N.; Kumari, H.L.J.; Singaravelu, C.M.; Kandasamy, R.; Kandasamy, J. Physicochemical investigations of biogenic chitosan-silver nanocomposite as antimicrobial and anticancer agent. *Int. J. Biol. Macromol.* **2016**, *92*, 77–87.
122. Estrela-Llopis, V.R.; Chevichalova, A.V.; Trigubova, N.A.; Ryzhuk, E.V. Heterocoagulation of polysaccharide-coated platinum nanoparticles with ovarian-cancer cells. *Colloid J.* **2014**, *76*, 609–621.
123. Jia, X.; Liu, Q.; Zou, S.; Xu, X.; Zhang, L. Construction of selenium nanoparticles/ $\beta$ -glucan composites for enhancement of the antitumor activity. *Carbohydr. Polym.* **2015**, *117*, 434–442.
124. Ren, Y.; Zhao, T.; Mao, G.; Zhang, M.; Li, F.; Zou, Y.; Yang, L.; Wu, X. Antitumor activity of hyaluronic acid-selenium nanoparticles in Heps tumor mice models. *Int. J. Biol. Macromol.* **2013**, *57*, 57–62.
125. Chen, T.; Wong, Y.S.; Zheng, W.; Bai, Y.; Huang, L. Selenium nanoparticles fabricated in *Undaria pinnatifida* polysaccharide solutions induce mitochondria-mediated apoptosis in A375 human melanoma cells. *Colloids Surf. B Biointerfaces* **2008**, *67*, 26–31.

126. Yang, F.; Tang, Q.; Zhong, X.; Bai, Y.; Chen, T.; Zhang, Y.; Li, Y.; Zheng, W. Surface decoration by *Spirulina* polysaccharide enhances the cellular uptake and anticancer efficacy of selenium nanoparticles. *Int. J. Nanomed.* **2012**, *7*, 835–844.
127. Wu, H.; Li, X.; Liu, W.; Chen, T.; Li, Y.; Zheng, W.; Man, C.W.-Y.; Wong, M.-K.; Wong, K.-H. Surface decoration of selenium nanoparticles by mushroom polysaccharides–protein complexes to achieve enhanced cellular uptake and antiproliferative activity. *J. Mater. Chem.* **2012**, *22*, 9602–9610.
128. Martin, C.; Low, W.L.; Amin, M.C.I.M.; Radecka, I.; Raj, P.; Kenward, K. Current trends in the development of wound dressings, biomaterials and devices. *Pharm. Pat. Anal.* **2013**, *2*, 341–359.
129. El-Feky, G.S.; Sharaf, S.S.; El Shafei, A.; Hegazy, A.A. Using chitosan nanoparticles as drug carriers for the development of a silver sulfadiazine wound dressing. *Carbohydr. Polym.* **2017**, *158*, 11–19.
130. Kamoun, E.A.; Chen, X.; Mohy Eldin, M.S.; Kenawy, E.R.S. Crosslinked poly(vinyl alcohol) hydrogels for wound dressing applications: A review of remarkably blended polymers. *Arab. J. Chem.* **2015**, *8*, 1–14.
131. Keleştemur, S.; Kilic, E.; Uslu, Ü.; Cumbul, A.; Ugur, M.; Akman, S.; Culha, M. Wound healing properties of modified silver nanoparticles and their distribution in mouse organs after topical application. *Nano Biomed. Eng.* **2012**, *4*, 170–176.
132. Mugade, M.; Patole, M.; Pokharkar, V. Bioengineered mannan sulphate capped silver nanoparticles for accelerated and targeted wound healing: Physicochemical and biological investigations. *Biomed. Pharmacother.* **2017**, *91*, 95–110.
133. Huang, J.; Ren, J.; Chen, G.; Deng, Y.; Wang, G.; Wu, X. Evaluation of the Xanthan-Based Film Incorporated with Silver Nanoparticles for Potential Application in the Nonhealing Infectious Wound. *J. Nanomater.* **2017**, *2017*, 6802397.
134. Singla, R.; Soni, S.; Patial, V.; Kulurkar, P.M.; Kumari, A.; Mahesh, S.; Padwad, Y.S.; Yadav, S.K. In vivo diabetic wound healing potential of nanobiocomposites containing bamboo cellulose nanocrystals impregnated with silver nanoparticles. *Int. J. Biol. Macromol.* **2017**, *105*, 45–55, doi:10.1016/j.ijbiomac.2017.06.109.
135. Haseeb, M.T.; Hussain, M.A.; Abbas, K.; Youssif, B.G.M.; Bashir, S.; Yuk, S.H.; Bukhari, S.N.A. Linseed hydrogel-mediated green synthesis of silver nanoparticles for antimicrobial and wound-dressing applications. *Int. J. Nanomed.* **2017**, *12*, 2845–2855.
136. Gupta, A.; Low, W.L.; Radecka, I.; Britland, S.T.; Mohd Amin, M.C.I.; Martin, C. Characterisation and in vitro antimicrobial activity of biosynthetic silver-loaded bacterial cellulose hydrogels. *J. Microencapsul.* **2016**, *33*, 725–734.
137. Muhammad, G.; Hussain, M.A.; Amin, M.; Hussain, S.Z.; Hussain, I.; Abbas Bukhari, S.N.; Naeem-ul-Hassan, M. Glucuronoxylan-mediated silver nanoparticles: Green synthesis, antimicrobial and wound healing applications. *RSC Adv.* **2017**, *7*, 42900–42908.
138. Ding, L.; Shan, X.; Zhao, X.; Zha, H.; Chen, X.; Wang, J.; Cai, C.; Wang, X.; Li, G.; Hao, J.; et al. Spongy bilayer dressing composed of chitosan–Ag nanoparticles and chitosan–Bletilla striata polysaccharide for wound healing applications. *Carbohydr. Polym.* **2017**, *157*, 1538–1547.
139. Mulens, V.; Morales, M.D.P.; Barber, D.F.; Barber, D.F. Development of Magnetic Nanoparticles for Cancer Gene Therapy: A Comprehensive Review. *ISRN Nanomater.* **2013**, *2013*, 1–14.
140. Venkatesan, J.; Anil, S.; Kim, S.-K.; Shim, M. Seaweed Polysaccharide-Based Nanoparticles: Preparation and Applications for Drug Delivery. *Polymers* **2016**, *8*, 30.
141. Maiyo, F.; Singh, M. Selenium nanoparticles: Potential in cancer gene and drug delivery. *Nanomedicine* **2017**, *12*, 1075–1089, doi:10.2217/nnm-2017-0024.
142. Manivasagan, P.; Bharathiraja, S.; Bui, N.Q.; Jang, B.; Oh, Y.O.; Lim, I.G.; Oh, J. Doxorubicin-loaded fucoidan capped gold nanoparticles for drug delivery and photoacoustic imaging. *Int. J. Biol. Macromol.* **2016**, *91*, 578–588.
143. Manivasagan, P.; Bharathiraja, S.; Bui, N.Q.; Lim, I.G.; Oh, J. Paclitaxel-loaded chitosan oligosaccharide-stabilized gold nanoparticles as novel agents for drug delivery and photoacoustic imaging of cancer cells. *Int. J. Pharm.* **2016**, *511*, 367–379.
144. Li, N.; Chen, Y.; Zhang, Y.-M.; Yang, Y.; Su, Y.; Chen, J.-T.; Liu, Y. Polysaccharide-Gold Nanocluster Supramolecular Conjugates as a Versatile Platform for the Targeted Delivery of Anticancer Drugs. *Sci. Rep.* **2015**, *4*, 4164.
145. Aryal, S.; Grailer, J.J.; Pilla, S.; Steeber, D.A.; Gong, S. Doxorubicin conjugated gold nanoparticles as water-soluble and pH-responsive anticancer drug nanocarriers. *J. Mater. Chem.* **2009**, *19*, 7879–7884.

146. Reddy, P.R.S.; Eswaramma, S.; Rao, K.S.V.K.; Lee, Y.I. Dual responsive pectin hydrogels and their silver nanocomposites: Swelling studies, controlled drug delivery and antimicrobial applications. *Bull. Korean Chem. Soc.* **2014**, *35*, 2391–2399.
147. Rau, L.R.; Tsao, S.W.; Liaw, J.W.; Tsai, S.W. Selective Targeting and Restrictive Damage for Nonspecific Cells by Pulsed Laser-Activated Hyaluronan-Gold Nanoparticles. *Biomacromolecules* **2016**, *17*, 2514–2521.
148. Jiang, W.; Fu, Y.; Yang, F.; Yang, Y.; Liu, T.; Zheng, W.; Zeng, L.; Chen, T. Gracilaria lemaneiformis polysaccharide as integrin-targeting surface decorator of selenium nanoparticles to achieve enhanced anticancer efficacy. *ACS Appl. Mater. Interfaces* **2014**, *6*, 13738–13748.
149. Silva-Cunha, A.; Chéron, M.; Grossiord, J.L.; Puisieux, F.; Seiller, M. W/O/W multiple emulsions of insulin containing a protease inhibitor and an absorption enhancer: Biological activity after oral administration to normal and diabetic rats. *Int. J. Pharm.* **1998**, *169*, 33–44.
150. Bhumkar, D.R.; Joshi, H.M.; Sastry, M.; Pokharkar, V.B. Chitosan reduced gold nanoparticles as novel carriers for transmucosal delivery of insulin. *Pharm. Res.* **2007**, *24*, 1415–1426.
151. Kievit, F.M.; Veisoh, O.; Bhattarai, N.; Fang, C.; Gunn, J.W.; Lee, D.; Ellenbogen, R.G.; Olson, J.M.; Zhang, M. PEI-PEG-chitosan-copolymer-coated iron oxide nanoparticles for safe gene delivery: Synthesis, complexation, and transfection. *Adv. Funct. Mater.* **2009**, *19*, 2244–2251.
152. Chen, T.; Xu, S.; Zhao, T.; Zhu, L.; Wei, D.; Li, Y.; Zhang, H.; Zhao, C. Gold nanocluster-conjugated amphiphilic block copolymer for tumor-targeted drug delivery. *ACS Appl. Mater. Interfaces* **2012**, *4*, 5766–5774.
153. Safari, D.; Marradi, M.; Chiodo, F.; Th Dekker, H.A.; Shan, Y.; Adamo, R.; Oscarson, S.; Rijkers, G.T.; Lahmann, M.; Kamerling, J.P.; et al. Gold nanoparticles as carriers for a synthetic Streptococcus pneumoniae type 14 conjugate vaccine. *Nanomedicine* **2012**, *7*, 651–662.
154. Rastegari, B.; Karbalaie-Heidari, H.R.; Zeinali, S.; Sheardown, H. The enzyme-sensitive release of prodigiosin grafted  $\beta$ -cyclodextrin and chitosan magnetic nanoparticles as an anticancer drug delivery system: Synthesis, characterization and cytotoxicity studies. *Colloids Surf. B Biointerfaces* **2017**, *158*, 589–601.
155. Pooja, D.; Panyaram, S.; Kulhari, H.; Reddy, B.; Rachamalla, S.S.; Sistla, R. Natural polysaccharide functionalized gold nanoparticles as biocompatible drug delivery carrier. *Int. J. Biol. Macromol.* **2015**, *80*, 48–56.
156. Cai, H.; Yao, P. In situ preparation of gold nanoparticle-loaded lysozyme-dextran nanogels and applications for cell imaging and drug delivery. *Nanoscale* **2013**, *5*, 2892–2900.
157. Vu-Quang, H.; Yoo, M.K.; Jeong, H.J.; Lee, H.J.; Muthiah, M.; Rhee, J.H.; Lee, J.H.; Cho, C.S.; Jeong, Y.Y.; Park, I.K. Targeted delivery of mannan-coated superparamagnetic iron oxide nanoparticles to antigen-presenting cells for magnetic resonance-based diagnosis of metastatic lymph nodes in vivo. *Acta Biomater.* **2011**, *7*, 3935–3945.
158. Yoo, M.K.; Park, I.Y.K.; Kim, I.Y.; Kwon, J.S.; Jeong, H.J.; Jeong, Y.Y.; Cho, C.S. Superparamagnetic iron oxide nanoparticles coated with mannan for macrophage targeting. *J. Nanosci. Nanotechnol.* **2008**, *8*, 5196–5202.
159. Chichova, M.; Shkodrova, M.; Vasileva, P.; Kirilova, K.; Doncheva-Stoimenova, D. Influence of silver nanoparticles on the activity of rat liver mitochondrial ATPase. *J. Nanopart. Res.* **2014**, *16*, 2243.
160. Mahdavinia, G.R.; Mosallanezhad, A.; Soleymani, M.; Sabzi, M. Magnetic- and pH-responsive  $\kappa$ -carrageenan/chitosan complexes for controlled release of methotrexate anticancer drug. *Int. J. Biol. Macromol.* **2017**, *97*, 209–217.
161. Assa, F.; Jafarizadeh-Malmiri, H.; Ajamein, H.; Anarjan, N.; Vaghari, H.; Sayyar, Z.; Berenjian, A. A biotechnological perspective on the application of iron oxide nanoparticles. *Nano Res.* **2016**, *9*, 2203–2225.
162. Taton, T.A. Scanometric DNA Array Detection with Nanoparticle Probes. *Science* **2000**, *289*, 1757–1760.
163. Tagad, C.K.; Kim, H.U.; Aiyer, R.C.; More, P.; Kim, T.; Moh, S.H.; Kulkarni, A.; Sabharwal, S.G. A sensitive hydrogen peroxide optical sensor based on polysaccharide stabilized silver nanoparticles. *RSC Adv.* **2013**, *3*, 22940–22943.
164. Tagad, C.K.; Dugasani, S.R.; Aiyer, R.; Park, S.; Kulkarni, A.; Sabharwal, S. Green synthesis of silver nanoparticles and their application for the development of optical fiber based hydrogen peroxide sensor. *Sens. Actuators B Chem.* **2013**, *183*, 144–149.
165. Narayanan, K.B.; Han, S.S. Colorimetric detection of manganese (II) ions using alginate-stabilized silver nanoparticles. *Res. Chem. Intermed.* **2017**, *43*, 5665–5674.
166. Bankura, K.; Rana, D.; Mollick, M.M.R.; Pattanayak, S.; Bhowmick, B.; Saha, N.R.; Roy, I.; Midya, T.; Barman, G.; Chattopadhyay, D. Dextrin-mediated synthesis of Ag NPs for colorimetric assays of Cu<sup>2+</sup> ion and Au NPs for catalytic activity. *Int. J. Biol. Macromol.* **2015**, *80*, 309–316.

167. Guan, H.; Yu, J.; Chi, D. Label-free colorimetric sensing of melamine based on chitosan-stabilized gold nanoparticles probes. *Food Control* **2013**, *32*, 35–41.
168. Narasimhan, L.R.; Goodman, W.; Patel, C.K.N. Correlation of breath ammonia with blood urea nitrogen and creatinine during hemodialysis. *Proc. Natl. Acad. Sci. USA* **2001**, *98*, 4617–4621.
169. Pandey, S.; Goswami, G.K.; Nanda, K.K. Green synthesis of biopolymer-silver nanoparticle nanocomposite: An optical sensor for ammonia detection. *Int. J. Biol. Macromol.* **2012**, *51*, 583–589.
170. Pandey, S.; Goswami, G.K.; Nanda, K.K. Green synthesis of polysaccharide/gold nanoparticle nanocomposite: An efficient ammonia sensor. *Carbohydr. Polym.* **2013**, *94*, 229–234.
171. Pandey, S.; Nanda, K.K. Au Nanocomposite Based Chemiresistive Ammonia Sensor for Health Monitoring. *ACS Sens.* **2016**, *1*, 55–62.
172. Dai, Z.; Xu, L.; Duan, G.; Li, T.; Zhang, H.; Li, Y.; Wang, Y.; Wang, Y.; Cai, W. Fast-Response, Sensitivity and Low-Powered Chemosensors by Fusing Nanostructured Porous Thin Film and IDEs-Microheater Chip. *Sci. Rep.* **2013**, *3*, 1669.
173. Gattu, K.P.; Kashale, A.A.; Ghule, K.; Ingole, V.H.; Sharma, R.; Deshpande, N.G.; Ghule, A.V. NO<sub>2</sub> sensing studies of bio-green synthesized Au-doped SnO<sub>2</sub>. *J. Mater. Sci. Mater. Electron.* **2017**, *28*, 13209–13216.
174. Tagad, C.K.; Rajdeo, K.S.; Kulkarni, A.; More, P.; Aiyer, R.C.; Sabharwal, S.; Hu, J.; Cai, W.; Cai, W.; Calderer, J. Green synthesis of polysaccharide stabilized gold nanoparticles: Chemo catalytic and room temperature operable vapor sensing application. *RSC Adv.* **2014**, *4*, 24014–24019.
175. Davidović, S.; Lazić, V.; Vukoje, I.; Papan, J.; Anhrenkiel, S.P.; Dimitrijević, S.; Nedeljković, J.M. Dextran coated silver nanoparticles—Chemical sensor for selective cysteine detection. *Colloids Surf. B Biointerfaces* **2017**, *160*, doi:10.1016/j.colsurfb.2017.09.031.
176. Lee, K.C.; Chiang, H.L.; Chiu, W.R.; Chen, Y.C. Molecular recognition between insulin and dextran encapsulated gold nanoparticles. *J. Mol. Recognit.* **2016**, *29*, 528–535.
177. Lai, C.; Zeng, G.M.; Huang, D.L.; Zhao, M.H.; Wei, Z.; Huang, C.; Xu, P.; Li, N.J.; Zhang, C.; Chen, M.; et al. Synthesis of gold-cellobiose nanocomposites for colorimetric measurement of cellobiase activity. *Spectrochim. Acta Part A Mol. Biomol. Spectrosc.* **2014**, *132*, 369–374.
178. Shen, M.Y.; Chao, C.F.; Wu, Y.J.; Wu, Y.H.; Huang, C.P.; Li, Y.K. A design for fast and effective screening of hyaluronidase inhibitor using gold nanoparticles. *Sens. Actuators B Chem.* **2013**, *181*, 605–610.
179. Li, Q.; Sun, A.; Si, Y.; Chen, M.; Wu, L. One-Pot Synthesis of Polysaccharide-Diphenylalanine Ensemble with Gold Nanoparticles and Dye for Highly Efficient Detection of Glutathione. *Chem. Mater.* **2017**, *29*, 6758–6765.
180. Chen, Z.; Zhang, X.; Cao, H.; Huang, Y. Chitosan-capped silver nanoparticles as a highly selective colorimetric probe for visual detection of aromatic ortho-trihydroxy phenols. *Analyst* **2013**, *138*, 2343–2349.
181. Sergeev, A.A.; Mironenko, A.Y.; Nazirov, A.E.; Leonov, A.A.; Voznesenskii, S.S. Nanocomposite Polymer Structures for Optical Sensors of Hydrogen Sulfide. *Tech. Phys.* **2017**, *62*, 1277–1280.
182. Rastogi, P.K.; Ganesan, V.; Krishnamoorthi, S. Palladium nanoparticles decorated gaur gum based hybrid material for electrocatalytic hydrazine determination. *Electrochim. Acta* **2014**, *125*, 593–600.
183. Luo, Y.; Shen, S.; Luo, J.; Wang, X.; Sun, R. Green synthesis of silver nanoparticles in xylan solution via Tollens reaction and their detection for Hg<sup>2+</sup>. *Nanoscale* **2015**, *7*, 690–700.
184. Su, H.; Liu, Y.; Wang, D.; Wu, C.; Xia, C.; Gong, Q.; Song, B.; Ai, H. Amphiphilic starlike dextran wrapped superparamagnetic iron oxide nanoparticle clusters as effective magnetic resonance imaging probes. *Biomaterials* **2013**, *34*, 1193–1203.
185. Hemmati, B.; Javanshir, S.; Dolatkhan, Z. Hybrid magnetic Irish moss/Fe<sub>3</sub>O<sub>4</sub> as a nano-biocatalyst for synthesis of imidazopyrimidine derivatives. *RSC Adv.* **2016**, *6*, 50431–50436.
186. Lee, J.S.; Saka, S. Biodiesel production by heterogeneous catalysts and supercritical technologies. *Bioresour. Technol.* **2010**, *101*, 7191–7200.
187. Grunes, J.; Zhu, J.; Somorjai, G.A. Catalysis and nanoscience. *Chem. Commun.* **2003**, *18*, 2257–2260.
188. Králik, M.; Biffis, A. Catalysis by metal nanoparticles supported on functional organic polymers. *J. Mol. Catal. A Chem.* **2001**, *177*, 113–138.
189. Chang, Y.C.; Chen, D.H. Catalytic reduction of 4-nitrophenol by magnetically recoverable Au nanocatalyst. *J. Hazard. Mater.* **2009**, *165*, 664–669.
190. Aditya, T.; Pal, A.; Pal, T. Nitroarene reduction: A trusted model reaction to test nanoparticle catalysts. *Chem. Commun.* **2015**, *51*, 9410–9431.

191. Rode, C.V.; Vaidya, M.J.; Chaudhari, R.V. Synthesis of p-Aminophenol by Catalytic Hydrogenation of Nitrobenzene. *Org. Process Res. Dev.* **1999**, *3*, 465–470.
192. Zhou, J.; Gao, J.; Xu, X.; Hong, W.; Song, Y.; Xue, R.; Zhao, H.; Liu, Y.; Qiu, H. Synthesis of porous Bi@Cs networks by a one-step hydrothermal method and their superior catalytic activity for the reduction of 4-nitrophenol. *J. Alloys Compd.* **2017**, *709*, 206–212.
193. Zheng, Z.; Huang, Q.; Guan, H.; Liu, S. In situ synthesis of silver nanoparticles dispersed or wrapped by a *Cordyceps sinensis* exopolysaccharide in water and their catalytic activity. *RSC Adv.* **2015**, *5*, 69790–69799.
194. Gao, Z.; Su, R.; Huang, R.; Qi, W.; He, Z. Glucomannan-mediated facile synthesis of gold nanoparticles for catalytic reduction of 4-nitrophenol. *Nanoscale Res. Lett.* **2014**, *9*, 404.
195. Maity, S.; Sen, I.K.; Islam, S.S. Green synthesis of gold nanoparticles using gum polysaccharide of *Cochlospermum religiosum* (katira gum) and study of catalytic activity. *Phys. E Low-Dimens. Syst. Nanostruct.* **2012**, *45*, 130–134.
196. Tripathy, T.; Kolya, H.; Jana, S.; Senapati, M. Green synthesis of Ag-Au bimetallic nanocomposites using a biodegradable synthetic graft copolymer; hydroxyethyl starch-g-poly(acrylamide-co-acrylic acid) and evaluation of their catalytic activities. *Eur. Polym. J.* **2017**, *87*, 113–123.
197. Yang, Y.; Buchwald, S.L. Ligand-controlled palladium-catalyzed regiodivergent suzuki-miyaura cross-coupling of allylboronates and aryl halides. *J. Am. Chem. Soc.* **2013**, *135*, 10642–10645.
198. Elazab, H.A.; Siamaki, A.R.; Moussa, S.; Gupton, B.F.; El-Shall, M.S. Highly efficient and magnetically recyclable graphene-supported Pd/Fe<sub>3</sub>O<sub>4</sub> nanoparticle catalysts for Suzuki and Heck cross-coupling reactions. *Appl. Catal. A Gen.* **2015**, *491*, 58–69.
199. Chen, W.; Zhong, L.; Peng, X.; Lin, J.; Sun, R. Xylan-type hemicelluloses supported terpyridine-palladium(II) complex as an efficient and recyclable catalyst for Suzuki-Miyaura reaction. *Cellulose* **2014**, *21*, 125–137.
200. Chtchigrovsky, M.; Lin, Y.; Ouchaou, K.; Chaumontet, M.; Robitzer, M.; Quignard, F.; Taran, F. Dramatic effect of the gelling cation on the catalytic performances of alginate-supported palladium nanoparticles for the Suzuki-Miyaura reaction. *Chem. Mater.* **2012**, *24*, 1505–1510.
201. Arcon, I.; Paganelli, S.; Piccolo, O.; Gallo, M.; Vogel-Mikus, K.; Baldi, F. XAS analysis of iron and palladium bonded to a polysaccharide produced anaerobically by a strain of *Klebsiella oxytoca*. *J. Synchrotron Radiat.* **2015**, *22*, 1215–1226.
202. Paganelli, S.; Piccolo, O.; Baldi, F.; Tassini, R.; Gallo, M.; La Sorella, G. Aqueous biphasic hydrogenations catalyzed by new biogenerated Pd-polysaccharide species. *Appl. Catal. A Gen.* **2013**, *451*, 144–152.
203. Chook, S.W.; Chia, C.H.; Chan, C.H.; Chin, S.X.; Zakaria, S.; Sajab, M.S.; Huang, N.M. A porous aerogel nanocomposite of silver nanoparticles-functionalized cellulose nanofibrils for SERS detection and catalytic degradation of rhodamine B. *RSC Adv.* **2015**, *5*, 88915–88920.
204. Lin, S.T.; Thirumavalavan, M.; Jiang, T.Y.; Lee, J.F. Synthesis of ZnO/Zn nano photocatalyst using modified polysaccharides for photodegradation of dyes. *Carbohydr. Polym.* **2014**, *105*, 1–9.
205. Cheryl-Low, Y.L.; Theam, K.L.; Lee, H.V. Alginate-derived solid acid catalyst for esterification of low-cost palm fatty acid distillate. *Energy Convers. Manag.* **2015**, *106*, 932–940.
206. Sherly, K.B.; Rakesh, K. Synthesis and catalytic activity of polysaccharide templated nanocrystalline sulfated zirconia. *AIP Conf. Proc.* **2014**, *128*, 128–131.
207. Behar, S.; Gonzalez, P.; Agulhon, P.; Quignard, F.; Świerczyński, D. New synthesis of nanosized Cu-Mn spinels as efficient oxidation catalysts. *Catal. Today* **2012**, *189*, 35–41.
208. Porta, F.; Rossi, M. Gold nanostructured materials for the selective liquid phase catalytic oxidation. *J. Mol. Catal. A Chem.* **2003**, *204–205*, 553–559.
209. Wang, Y.; Kong, Q.; Ding, B.; Chen, Y.; Yan, X.; Wang, S.; Chen, F.; You, J.; Li, C. Bioinspired catecholic activation of marine chitin for immobilization of Ag nanoparticles as recyclable pollutant nanocatalysts. *J. Colloid Interface Sci.* **2017**, *505*, 220–229.
210. Pourjavadi, A.; Motamedi, A.; Marvdashti, Z.; Hosseini, S.H. Magnetic nanocomposite based on functionalized salep as a green support for immobilization of palladium nanoparticles: Reusable heterogeneous catalyst for Suzuki coupling reactions. *Catal. Commun.* **2017**, *97*, 27–31.
211. Li, Y.; Li, G.; Li, W.; Yang, F.; Liu, H. Greenly Synthesized Gold-Alginate Nanocomposites Catalyst for Reducing Decoloration of Azo-Dyes. *Nano* **2015**, *10*, 1550108.
212. Lee, Y.J.; Cha, S.-H.; Lee, K.J.; Kim, Y.S.; Cho, S.; Park, Y. Plant Extract (*Bupleurum falcatum*) as a Green Factory for Biofabrication of Gold Nanoparticles. *Nat. Prod. Commun.* **2015**, *10*, 1593–1596.



213. Ahmed, K.B.A.; Kalla, D.; Uppuluri, K.B.; Anbazhagan, V. Green synthesis of silver and gold nanoparticles employing levan, a biopolymer from *Acetobacter xylinum* NCIM 2526, as a reducing agent and capping agent. *Carbohydr. Polym.* **2014**, *112*, 539–545.
214. Thirumavalavan, M.; Yang, F.M.; Lee, J.F. Investigation of preparation conditions and photocatalytic efficiency of nano ZnO using different polysaccharides. *Environ. Sci. Pollut. Res.* **2013**, *20*, 5654–5664.
215. Sen, I.K.; Maity, K.; Islam, S.S. Green synthesis of gold nanoparticles using a glucan of an edible mushroom and study of catalytic activity. *Carbohydr. Polym.* **2013**, *91*, 518–528.
216. Budarin, V.L.; Clark, J.H.; Luque, R.; Macquarrie, D.J.; White, R.J. Palladium nanoparticles on polysaccharide-derived mesoporous materials and their catalytic performance in C–C coupling reactions. *Green Chem.* **2008**, *10*, 382–387.
217. Yah, C.S.; Iyuke, S.E.; Simate, G.S. A review of nanoparticles toxicity and their routes of exposures. *Iran. J. Pharm. Sci.* **2012**, *8*, 299–314.
218. Medina, C.; Santos-Martinez, M.J.; Radomski, A.; Corrigan, O.I.; Radomski, M.W. Nanoparticles: Pharmacological and toxicological significance. *Br. J. Pharmacol.* **2009**, *150*, 552–558.
219. Lam, C.-W.; James, J.T.; McCluskey, R.; Hunter, R.L. Pulmonary toxicity of single-wall carbon nanotubes in mice 7 and 90 days after intratracheal instillation. *Toxicol. Sci.* **2004**, *77*, 126–134.
220. Radomski, A.; Jurasz, P.; Alonso-Escolano, D.; Drews, M.; Morandi, M.; Malinski, T.; Radomski, M.W. Nanoparticle-induced platelet aggregation and vascular thrombosis. *Br. J. Pharmacol.* **2005**, *146*, 882–893.
221. Hussain, S.M.; Javorina, A.K.; Schrand, A.M.; Duhart, H.M.H.M.; Ali, S.F.; Schlager, J.J. The interaction of manganese nanoparticles with PC-12 cells induces dopamine depletion. *Toxicol. Sci.* **2006**, *92*, 456–463.
222. Xie, J.-H.; Jin, M.-L.; Morris, G.A.; Zha, X.-Q.; Chen, H.-Q.; Yi, Y.; Li, J.-E.; Wang, Z.-J.; Gao, J.; Nie, S.-P.; et al. Advances on Bioactive Polysaccharides from Medicinal Plants. *Crit. Rev. Food Sci. Nutr.* **2016**, *56*, S60–S84.
223. Berry, J.; Arnoux, B.; Stanislas, G.; Galle, P.; Chretien, J. A microanalytic study of particles transport across the alveoli: Role of blood platelets. *Biomedicine* **1977**, *27*, 354–357.
224. Nemmar, A.; Hoet, P.H.M.; Vanquickenborne, B.; Dinsdale, D.; Thomeer, M.; Hoylaerts, M.F.; Vanbilloen, H.; Mortelmans, L.; Nemery, B. Passage of inhaled particles into the blood circulation in humans. *Circulation* **2002**, *105*, 411–414.
225. Pooja, D.; Panyaram, S.; Kulhari, H.; Rachamalla, S.S.; Sistla, R. Xanthan gum stabilized gold nanoparticles: Characterization, biocompatibility, stability and cytotoxicity. *Carbohydr. Polym.* **2014**, *110*, 1–9.
226. Asharani, P.V.; Sethu, S.; Vadukumpully, S.; Zhong, S.; Lim, C.T.; Hande, M.P.; Valiyaveetil, S. Investigations on the structural damage in human erythrocytes exposed to silver, gold, and platinum nanoparticles. *Adv. Funct. Mater.* **2010**, *20*, 1233–1242.
227. Dhar, S.; Murawala, P.; Shiras, A.; Pokharkar, V.; Prasad, B.L.V. Gellan gum capped silver nanoparticle dispersions and hydrogels: Cytotoxicity and in vitro diffusion studies. *Nanoscale* **2012**, *4*, 563–567.
228. Amorim, M.O.R.; Gomes, D.L.; Dantas, L.A.; Viana, R.L.S.; Chiquetti, S.C.; Almeida-Lima, J.; Silva Costa, L.; Rocha, H.A.O. Fucan-coated silver nanoparticles synthesized by a green method induce human renal adenocarcinoma cell death. *Int. J. Biol. Macromol.* **2016**, *93*, 57–65.
229. Venkatpurwar, V.; Mali, V.; Bodhankar, S.; Pokharkar, V. In vitro cytotoxicity and *in vivo* sub-acute oral toxicity assessment of porphyrin reduced gold nanoparticles. *Toxicol. Environ. Chem.* **2012**, *94*, 1357–1367.
230. Reena, K.; Balashanmugam, P.; Gajendiran, M.; Antony, S.A. Synthesis of Leucas Aspera Extract Loaded Gold-PLA-PEG-PLA Amphiphilic Copolymer Nanoconjugates: In Vitro Cytotoxicity and Anti-Inflammatory Activity Studies. *J. Nanosci. Nanotechnol.* **2016**, *16*, 4762–4770.
231. Worthington, K.L.S.; Adamcakova-Dodd, A.; Wongrakpanich, A.; Mudunkotuwa, I.A.; Mapuskar, K.A.; Joshi, V.B.; Allan Guymon, C.; Spitz, D.R.; Grassian, V.H.; Thorne, P.S.; et al. Chitosan coating of copper nanoparticles reduces *in vitro* toxicity and increases inflammation in the lung. *Nanotechnology* **2013**, *24*, 395101.
232. Li; Muralikrishnan, S.; Ng, C.T.; Yung, L.Y.; Bay, B.H. Nanoparticle-induced pulmonary toxicity. *Exp. Biol. Med.* **2010**, *235*, 1025–1033.
233. Hwang, P.A.; Lin, X.Z.; Kuo, K.L.; Hsu, F.Y. Fabrication and cytotoxicity of fucoidan-cisplatin nanoparticles for macrophage and tumor cells. *Materials* **2017**, *10*, 291.
234. Braydich-Stolle, L.K.; Breitner, E.K.; Comfort, K.K.; Schlager, J.J.; Hussain, S.M. Dynamic characteristics of silver nanoparticles in physiological fluids: Toxicological implications. *Langmuir* **2014**, *30*, 15309–15316.

235. Borysov, A.; Krisanova, N.; Chunihiin, O.; Ostapchenko, L.; Pozdnyakova, N.; Borisova, T. A comparative study of neurotoxic potential of synthesized polysaccharide-coated and native ferritin-based magnetic nanoparticles. *Croat. Med. J.* **2014**, *55*, 195–205.
236. Iram, F.; Iqbal, M.S.; Athar, M.M.; Saeed, M.Z.; Yasmeen, A.; Ahmad, R. Glucoxyilan-mediated green synthesis of gold and silver nanoparticles and their phyto-toxicity study. *Carbohydr. Polym.* **2014**, *104*, 29–33.
237. Dhar, S.; Mali, V.; Bodhankar, S.; Shiras, A.; Prasad, B.L.V.; Pokharkar, V. Biocompatible gellan gum-reduced gold nanoparticles: Cellular uptake and subacute oral toxicity studies. *J. Appl. Toxicol.* **2011**, *31*, 411–420.
238. Devendiran, R.M.; Chinnaiyan, S. kumar; Yadav, N.K.; Moorthy, G.K.; Ramanathan, G.; Singaravelu, S.; Sivagnanam, U.T.; Perumal, P.T. Green synthesis of folic acid-conjugated gold nanoparticles with pectin as reducing/stabilizing agent for cancer theranostics. *RSC Adv.* **2016**, *6*, 29757–29768.
239. Baroli, B.; Ennas, M.G.; Loffredo, F.; Isola, M.; Pinna, R.; López-Quintela, M.A. Penetration of metallic nanoparticles in human full-thickness skin. *J. Investig. Dermatol.* **2007**, *127*, 1701–1712.



© 2017 by the authors. Licensee MDPI, Basel, Switzerland. This article is an open access article distributed under the terms and conditions of the Creative Commons Attribution (CC BY) license (<http://creativecommons.org/licenses/by/4.0/>).